



# Suppression and azimuthal anisotropy of prompt and nonprompt $J/\psi$ production in PbPb collisions at $\sqrt{s_{NN}} = 2.76$ TeV

CMS Collaboration\*

CERN, 1211 Geneva 23, Switzerland

Received: 3 October 2016 / Accepted: 21 March 2017 / Published online: 19 April 2017

© CERN for the benefit of the CMS collaboration 2017. This article is an open access publication

**Abstract** The nuclear modification factor  $R_{AA}$  and the azimuthal anisotropy coefficient  $v_2$  of prompt and nonprompt (i.e. those from decays of b hadrons)  $J/\psi$  mesons, measured from PbPb and pp collisions at  $\sqrt{s_{NN}} = 2.76$  TeV at the LHC, are reported. The results are presented in several event centrality intervals and several kinematic regions, for transverse momenta  $p_T > 6.5$  GeV/c and rapidity  $|y| < 2.4$ , extending down to  $p_T = 3$  GeV/c in the  $1.6 < |y| < 2.4$  range. The  $v_2$  of prompt  $J/\psi$  is found to be nonzero, but with no strong dependence on centrality, rapidity, or  $p_T$  over the full kinematic range studied. The measured  $v_2$  of nonprompt  $J/\psi$  is consistent with zero. The  $R_{AA}$  of prompt  $J/\psi$  exhibits a suppression that increases from peripheral to central collisions but does not vary strongly as a function of either  $y$  or  $p_T$  in the fiducial range. The nonprompt  $J/\psi$   $R_{AA}$  shows a suppression which becomes stronger as rapidity or  $p_T$  increases. The  $v_2$  and  $R_{AA}$  of open and hidden charm, and of open charm and beauty, are compared.

## 1 Introduction

Recent data from RHIC and the CERN LHC for mesons containing charm and beauty quarks have allowed more detailed theoretical and experimental studies [1] of the phenomenology of these heavy quarks in a deconfined quark gluon plasma (QGP) [2] at large energy densities and high temperatures [3]. Heavy quarks, whether as quarkonium states  $Q\bar{Q}$  (hidden heavy flavour) [4] or as mesons made of heavy-light quark–antiquark pairs  $Q\bar{q}$  (open heavy flavour) [5], are considered key probes of the QGP, since their short formation time allows them to probe all stages of the QGP evolution [1].

At LHC energies, the inclusive  $J/\psi$  yield contains a significant nonprompt contribution from b hadron decays [6–8], offering the opportunity of studying both open beauty and hidden charm in the same measurement. Because of the long lifetime ( $\mathcal{O}(500)$   $\mu\text{m}/c$ ) of b hadrons, compared to the QGP

lifetime ( $\mathcal{O}(10)$   $fm/c$ ), the nonprompt contribution should not suffer from colour screening of the potential between the  $Q$  and the  $\bar{Q}$  by the surrounding light quarks and gluons, which decreases the prompt quarkonium yield [9]. Instead, the nonprompt contribution should reflect the energy loss of b quarks in the medium. The importance of an unambiguous and detailed measurement of open beauty flavour is driven by the need to understand key features of the dynamics of parton interactions and hadron formation in the QGP: the colour-charge and parton-mass dependences for the in-medium interactions [5, 10–13], the relative contribution of radiative and collisional energy loss [14–16], and the effects of different hadron formation times [17, 18]. Another aspect of the heavy-quark phenomenology in the QGP concerns differences in the behaviour (energy loss mechanisms, amount and strength of interactions with the surrounding medium) of a  $Q\bar{Q}$  pair (the pre-quarkonium state) relative to that of a single heavy quark  $Q$  (the pre-meson component) [19–21].

Experimentally, modifications to the particle production are usually quantified by the ratio of the yield measured in heavy ion collisions to that in proton–proton (pp) collisions, scaled by the mean number of binary nucleon–nucleon (NN) collisions. This ratio is called the nuclear modification factor  $R_{AA}$ . In the absence of medium effects, one would expect  $R_{AA} = 1$  for hard processes, which scale with the number of NN collisions. The  $R_{AA}$  for prompt and nonprompt  $J/\psi$  have been previously measured in PbPb at  $\sqrt{s_{NN}} = 2.76$  TeV by CMS in bins of transverse momentum ( $p_T$ ), rapidity ( $y$ ) and collision centrality [22]. A strong centrality-dependent suppression has been observed for  $J/\psi$  with  $p_T > 6.5$  GeV/c. The ALICE Collaboration has measured  $J/\psi$  down to  $p_T = 0$  GeV/c in the electron channel at midrapidity ( $|y| < 0.8$ ) [23] and in the muon channel at forward rapidity ( $2.5 < y < 4$ ) [24]. Except for the most peripheral event selection, a suppression of inclusive  $J/\psi$  meson production is observed for all collision centralities. However, the suppression is smaller than that at  $\sqrt{s_{NN}} = 0.2$  TeV [25], smaller at midrapidity than at forward rapidity, and, in the forward region, smaller for  $p_T < 2$  GeV/c than

\* e-mail: [cms-publication-committee-chair@cern.ch](mailto:cms-publication-committee-chair@cern.ch)

for  $5 < p_T < 8 \text{ GeV}/c$  [26]. All these results were interpreted as evidence that the measured prompt  $J/\psi$  yield is the result of an interplay between (a) primordial production ( $J/\psi$  produced in the initial hard-scattering of the collisions), (b) colour screening and energy loss ( $J/\psi$  destroyed or modified by interactions with the surrounding medium), and (c) recombination/regeneration mechanisms in a deconfined partonic medium, or at the time of hadronization ( $J/\psi$  created when a free charm and a free anti-charm quark come close enough to each other to form a bound state) [27–29].

A complement to the  $R_{AA}$  measurement is the elliptic anisotropy coefficient  $v_2$ . This is the second Fourier coefficient in the expansion of the azimuthal angle ( $\Phi$ ) distribution of the  $J/\psi$  mesons,  $dN/d\Phi \propto 1 + 2v_2 \cos[2(\Phi - \Psi_{PP})]$  with respect to  $\Psi_{PP}$ , the azimuthal angle of the “participant plane” calculated for each event. In a noncentral heavy ion collision, the overlap region of the two colliding nuclei has a lenticular shape. The participant plane is defined by the beam direction and the direction of the shorter axis of the lenticular region. Typical sources for a nonzero elliptic anisotropy are a path length difference arising from energy loss of particles traversing the reaction zone, or different pressure gradients along the short and long axes. Both effects convert the initial spatial anisotropy into a momentum anisotropy  $v_2$  [30]. The effect of energy loss is usually studied using high  $p_T$  and/or heavy particles (so-called “hard probes” of the medium), for which the parent parton is produced at an early stage of the collision. If the partons are emitted in the direction of the participant plane, they have on average a shorter in-medium path length than partons emitted orthogonally, leading to a smaller modification to their energy or, in the case of  $Q\bar{Q}$  and the correspondingonium state, a smaller probability of being destroyed. Pressure gradients drive in-medium interactions that can modify the direction of the partons. This effect is most important at low  $p_T$ .

The  $v_2$  of open charm (D mesons) and hidden charm (inclusive  $J/\psi$  mesons) was measured at the LHC by the ALICE Collaboration. The D mesons with  $2 < p_T < 6 \text{ GeV}/c$  [31] were found to have a significant positive  $v_2$ , while for  $J/\psi$  mesons with  $2 < p_T < 4 \text{ GeV}/c$  there was an indication of nonzero  $v_2$  [32]. The precision of the results does not yet allow a determination of the origin of the observed anisotropy. One possible interpretation is that charm quarks at low  $p_T$ , despite their much larger mass than those of the  $u$ ,  $s$ ,  $d$  quarks, participate in the collective expansion of the medium. A second possibility is that there is no collective motion for the charm quarks, and the observed anisotropy is acquired via quark recombination [27,33,34].

In this paper, the  $R_{AA}$  and the  $v_2$  for prompt and non-prompt  $J/\psi$  mesons are presented in several event centrality intervals and several kinematic regions. The results are based on event samples collected during the 2011 PbPb and 2013 pp LHC runs at a nucleon–nucleon centre-of-mass

energy of 2.76 TeV, corresponding to integrated luminosities of  $152 \mu\text{b}^{-1}$  and  $5.4 \text{ pb}^{-1}$ , respectively.

## 2 Experimental setup and event selection

A detailed description of the CMS detector, together with a definition of the coordinate system and the relevant kinematic variables, can be found in Ref. [35]. The central feature of the CMS apparatus is a superconducting solenoid, of 6 m internal diameter and 15 m length. Within the field volume are the silicon tracker, the crystal electromagnetic calorimeter, and the brass and scintillator hadron calorimeter. The CMS apparatus also has extensive forward calorimetry, including two steel and quartz-fiber Cherenkov hadron forward (HF) calorimeters, which cover the range  $2.9 < |\eta_{\text{det}}| < 5.2$ , where  $\eta_{\text{det}}$  is measured from the geometrical centre of the CMS detector. The calorimeter cells, in the  $\eta$ - $\phi$  plane, form towers projecting radially outwards from close to the nominal interaction point. These detectors are used in the present analysis for the event selection, collision impact parameter determination, and measurement of the azimuthal angle of the participant plane.

Muons are detected in the pseudorapidity window  $|\eta| < 2.4$ , by gas-ionization detectors made of three technologies: drift tubes, cathode strip chambers, and resistive plate chambers, embedded in the steel flux-return yoke of the solenoid. The silicon tracker is composed of pixel detectors (three barrel layers and two forward disks on either side of the detector, made of 66 million  $100 \times 150 \mu\text{m}^2$  pixels) followed by microstrip detectors (ten barrel layers plus three inner disks and nine forward disks on either side of the detector, with strip pitch between 80 and  $180 \mu\text{m}$ ).

The measurements reported here are based on PbPb and pp events selected online (triggered) by a hardware-based dimuon trigger without an explicit muon momentum threshold (i.e. the actual threshold is determined by the detector acceptance and efficiency of the muon trigger). The same trigger logic was used during the pp and PbPb data taking periods.

In order to select a sample of purely inelastic hadronic PbPb (pp) collisions, the contributions from ultraperipheral collisions and noncollision beam background are removed offline, as described in Ref. [36]. Events are preselected if they contain a reconstructed primary vertex formed by at least two tracks and at least three (one in the case of pp events) HF towers on each side of the interaction point with an energy of at least 3 GeV deposited in each tower. To further suppress the beam-gas events, the distribution of hits in the pixel detector along the beam direction is required to be compatible with particles originating from the event vertex. These criteria select  $(97 \pm 3)\%$  ( $>99\%$ ) of inelastic hadronic PbPb (pp) collisions with negligible contamination

from non-hadronic interactions [36]. Using this efficiency it is calculated that the PbPb sample corresponds to a number of minimum bias (MB) events  $N_{\text{MB}} = (1.16 \pm 0.04) \times 10^9$ . The pp data set corresponds to an integrated luminosity of  $5.4 \text{ pb}^{-1}$  known to an accuracy of 3.7% from the uncertainty in the calibration based on a van der Meer scan [37]. The two data sets correspond to approximately the same number of elementary NN collisions.

Muons are reconstructed offline using tracks in the muon detectors (“standalone muons”) that are then matched to tracks in the silicon tracker, using an algorithm optimized for the heavy ion environment [38]. In addition, an iterative track reconstruction algorithm [39] is applied to the PbPb data, limited to regions defined by the standalone muons. The pp reconstruction algorithm includes an iterative tracking step in the full silicon tracker. The final parameters of the muon trajectory are obtained from a global fit of the standalone muon with a matching track in the silicon tracker.

The centrality of heavy ion collisions, i.e. the geometrical overlap of the incoming nuclei, is correlated to the energy released in the collisions. In CMS, centrality is defined as percentiles of the distribution of the energy deposited in the HFs. Using a Glauber model calculation as described in Ref. [36], one can estimate variables related to the centrality, such as the mean number of nucleons participating in the collisions ( $N_{\text{part}}$ ), the mean number of binary NN collisions ( $N_{\text{coll}}$ ), and the average nuclear overlap function ( $T_{\text{AA}}$ ) [40]. The latter is equal to the number of NN binary collisions divided by the NN cross section and can be interpreted as the NN-equivalent integrated luminosity per heavy ion collision, at a given centrality. In the following,  $N_{\text{part}}$  will be the variable used to show the centrality dependence of the measurements, while  $T_{\text{AA}}$  directly enters into the nuclear modification factor calculation. It should be noted that the PbPb hadronic cross section ( $7.65 \pm 0.42 \text{ b}$ ), computed with this Glauber simulation, results in an integrated luminosity of  $152 \pm 9 \mu\text{b}^{-1}$ , compatible within 1.2 sigma with the integrated luminosity based on the van der Meer scan, which has been evaluated to be  $166 \pm 8 \mu\text{b}^{-1}$ . All the  $R_{\text{AA}}$  results presented in the paper have been obtained using the  $N_{\text{MB}}$  event counting that is equivalent to  $152 \mu\text{b}^{-1}$  expressed in terms of integrated luminosity.

Several Monte Carlo (MC) simulated event samples are used to model the signal shapes and evaluate reconstruction, trigger, and selection efficiencies. Samples of prompt and nonprompt  $J/\psi$  are generated with PYTHIA 6.424 [41] and decayed with EVTGEN 1.3.0 [42], while the final-state bremsstrahlung is simulated with PHOTOS 2.0 [43]. The prompt  $J/\psi$  is simulated unpolarized, a scenario in good agreement with pp measurements [44–46]. For nonprompt  $J/\psi$ , the results are reported for the polarization predicted by EVTGEN, roughly  $\lambda_\theta = -0.4$ , however not a well-defined value, since in many  $B \rightarrow J/\psi X$  modes the spin alignment is

either forced by angular momentum conservation or given as input from measured values of helicity amplitudes in decays. If the acceptances were different in pp and PbPb, they would not perfectly cancel in the  $R_{\text{AA}}$ . This would be the case if, for instance, some physics processes (such as polarization or energy loss) would affect the measurement in PbPb collisions with a strong kinematic dependence within an analysis bin. As in previous analyses [47–50], such possible physics effects are not considered as systematic uncertainties, but a quantitative estimate of this effect for two extreme polarization scenarios can be found in Ref. [22]. In the PbPb case, the PYTHIA signal events are further embedded in heavy ion events generated with HYDJET 1.8 [51], at the level of detector hits and with matching vertices. The detector response was simulated with GEANT4 [52], and the resulting information was processed through the full event reconstruction chain, including trigger emulation.

### 3 Analysis

Throughout this analysis the same methods for signal extraction and corrections are used for both the pp and PbPb data.

#### 3.1 Corrections

For both  $R_{\text{AA}}$  and  $v_2$  results, correction factors are applied event-by-event to each dimuon, to account for inefficiencies in the trigger, reconstruction, and selection of the  $\mu^+\mu^-$  pairs. They were evaluated, using MC samples, in four dimensions ( $p_T$ , centrality,  $y$ , and  $L_{xyz}$ ) for the PbPb results, and in three-dimensions ( $p_T$ ,  $y$ , and  $L_{xyz}$ ) for the pp results. After checking that the efficiencies on the prompt and non-prompt  $J/\psi$  MC samples near  $L_{xyz} = 0$  are in agreement, two efficiency calculations are made. One calculation is made on the prompt  $J/\psi$  MC sample, as a function of  $p_T$ , in 10 rapidity intervals between  $y = -2.4$  and  $y = 2.4$ , and 4 centrality bins (0–10%, 10–20%, 20–40%, and 40–100%). For each  $y$  and centrality interval, the  $p_T$  dependence of the efficiency is smoothed by fitting it with a Gaussian error function. A second efficiency is calculated using the non-prompt  $J/\psi$  MC sample, as a function of  $L_{xyz}$ , in the same  $y$  binning, but for coarser  $p_T$  bins and for centrality 0–100%. This is done in two steps. The efficiency is first calculated as a function of  $L_{xyz}^{\text{true}}$ , and then converted into an efficiency versus measured  $L_{xyz}$ , using a 2D dispersion map of  $L_{xyz}^{\text{true}}$  vs.  $L_{xyz}$ . In the end, each dimuon candidate selected in data, with transverse momentum  $p_T$ , rapidity  $y$ , centrality  $c$ , and  $L_{xyz} = d$  (mm), is assigned an efficiency weight equal to

$$w = \text{efficiency}^{\text{prompt}J/\psi}(p_T, y, c, L_{xyz} = 0) \times \frac{\text{efficiency}^{\text{nonprompt}J/\psi}(p_T, y, L_{xyz} = d)}{\text{efficiency}^{\text{nonprompt}J/\psi}(p_T, y, L_{xyz} = 0)}. \quad (1)$$

The individual components of the MC efficiency (tracking reconstruction, standalone muon reconstruction, global muon fit, muon identification and selection, triggering) are cross-checked using single muons from  $J/\psi$  decays in simulated and collision data, with the *tag-and-probe* technique (T&P) [53]. For all but the tracking reconstruction, scaling factors (calculated as the ratios between the data and MC T&P obtained efficiencies), estimated as a function of the muon  $p_T$  in several muon pseudorapidity regions, are used to scale the dimuon MC-calculated efficiencies. They are applied event-by-event, as a weight, to each muon that passes all analysis selections and enter the mass and  $\ell_{J/\psi}$  distributions. The weights are similar for the pp and PbPb samples, and range from 1.02 to 0.6 for single muons with  $p_T > 4 - 5 \text{ GeV}/c$  and  $p_T < 3.5 \text{ GeV}/c$ , respectively. For the tracking efficiency, which is above 99% even in the case of PbPb events, the full difference between data and MC T&P results (integrated over all the kinematic region probed) is propagated as a global (common to all points) systematic uncertainty.

### 3.2 Signal extraction

The single-muon acceptance and identification criteria are the same as in Ref. [22]. Opposite-charge muon pairs, with invariant mass between 2.6 and 3.5  $\text{GeV}/c^2$ , are fitted with a common vertex constraint and are kept if the fit  $\chi^2$  probability is larger than 1%. Results are presented in up to six bins of absolute  $J/\psi$  meson rapidity (equally spaced between 0 and 2.4) integrated over  $p_T$  ( $6.5 < p_T < 30 \text{ GeV}/c$ ), up to six bins in  $p_T$  ([6.5, 8.5], [8.5, 9.5], [9.5, 11], [11, 13], [13, 16], [16, 30]  $\text{GeV}/c$ ) integrated over rapidity ( $|y| < 2.4$ ), and up to three additional low- $p_T$  bins ([3, 4.5], [4.5, 5.5], [5.5, 6.5]  $\text{GeV}/c$ ) at forward rapidity ( $1.6 < |y| < 2.4$ ). The lower  $p_T$  limit for which the results are reported is imposed by the detector acceptance, the muon reconstruction algorithm, and the selection criteria used in the analysis. The PbPb sample is split in bins of collision centrality, defined using fractions of the inelastic hadronic cross section where 0% denotes the most central collisions. This fraction is determined from the HF energy distribution [54]. The most central (highest HF energy deposit) and most peripheral (lowest HF energy deposit) centrality bins used in the analysis are 0–5% and 60–100%, and 0–10% and 50–100%, for prompt and nonprompt  $J/\psi$  results, respectively. The rest of the centrality bins are in increments of 5% up to 50% for the high  $p_T$  prompt  $J/\psi$  results integrated over  $y$ , and in increments of 10% for all other cases. The  $N_{\text{part}}$  values, computed for events with a flat centrality distribution, range from  $381 \pm 2$  in the 0–5% bin to  $14 \pm 2$  in the 60–100% bin. If the events would be distributed according to the number of NN collisions,  $N_{\text{coll}}$ , which is expected for initially produced hard probes, the average  $N_{\text{part}}$  would become 25 instead of 14 for

the most peripheral bin, and 41 instead of 22 in the case of the 50–100% bin. For the other finer bins, the difference is negligible (less than 3%).

The same method for signal extraction is used in both the  $v_2$  and the  $R_{AA}$  analyses, for both the PbPb and pp samples. The separation of prompt  $J/\psi$  mesons from those coming from b hadron decays relies on the measurement of a secondary  $\mu^+\mu^-$  vertex displaced from the primary collision vertex. The displacement  $\vec{r}$  between the  $\mu^+\mu^-$  vertex and the primary vertex is measured first. Then, the most probable decay length of b hadron in the laboratory frame [55] is calculated as

$$L_{xyz} = \frac{\hat{u}^T S^{-1} \vec{r}}{\hat{u}^T S^{-1} \hat{u}}, \quad (2)$$

where  $\hat{u}$  is the unit vector in the direction of the  $J/\psi$  meson momentum ( $\vec{p}$ ) and  $S$  is the sum of the primary and secondary vertex covariance matrices. From this quantity, the pseudo-proper decay length  $\ell_{J/\psi} = L_{xyz} m_{J/\psi} / p$  (which is the decay length of the  $J/\psi$  meson) is computed as an estimate of the b hadron decay length.

To measure the fraction of the  $J/\psi$  mesons coming from b hadron decays (the so-called *b fraction*), the invariant-mass spectrum of  $\mu^+\mu^-$  pairs and their  $\ell_{J/\psi}$  distribution are fitted sequentially in an extended unbinned maximum likelihood fit. The fits are performed for each  $p_T$ ,  $|y|$ , and centrality bin of the analysis, and in addition in the case of the PbPb  $v_2$  analysis, in four bins in  $|\Delta\phi| = |\phi - \Psi_2|$ , equally spaced between 0 and  $\pi/2$ . The second-order “event plane” angle  $\Psi_2$ , measured as explained below, corresponds to the event-by-event azimuthal angle of maximum particle density. It is an approximation of the participant plane angle  $\Psi_{PP}$ , which is not directly observable.

The fitting procedure is similar to the one used in earlier analyses of pp collisions at  $\sqrt{s} = 7 \text{ TeV}$  [56], and PbPb collisions at  $\sqrt{s_{NN}} = 2.76 \text{ TeV}$  [22]. The  $J/\psi$  meson mass distribution is modelled by the sum of a Gaussian function and a Crystal Ball (CB) function [57], with a common mean  $m_0$  and independent widths. The CB radiative tail parameters are fixed to the values obtained in fits to simulated distributions for different kinematic regions [50]. The invariant mass background probability density function (PDF) is an exponential function whose parameters are allowed to float in each fit. Since the mass resolution depends on  $y$  and  $p_T$ , all resolution-related parameters are left free when binning as a function of  $|y|$  or  $p_T$ . In the case of centrality binning, the width of the CB function is left free, while the rest of the parameters are fixed to the centrality-integrated results, 0–100%, for a given  $p_T$  and  $|y|$  bin. When binning in  $|\Delta\phi|$ , all signal parameters are fixed to their values in the  $|\Delta\phi|$ -integrated fit.



The  $\ell_{J/\psi}$  distribution is modeled by a prompt signal component represented by a resolution function, a nonprompt component given by an exponential function convoluted with the resolution function, and the continuum background component represented by the sum of the resolution function plus three exponential decay functions to take into account long-lived background components [56]. The resolution function is comprised of the sum of two Gaussian functions, which depend upon the per-event uncertainty of the measured  $\ell_{J/\psi}$ , determined from the covariance matrices of the primary and secondary vertex fits. The fit parameters of the  $\ell_{J/\psi}$  distribution were determined through a series of fits. Pseudo-proper decay length background function parameters are fixed using dimuon events in data located on each side of the  $J/\psi$  resonance peak. In all cases, the b fraction is a free fit parameter. An example of 2D fits is given in Fig. 1.

The  $v_2$  analysis follows closely the event plane method described in Ref. [58]. The  $J/\psi$  mesons reconstructed with  $y > 0$  ( $y < 0$ ) are correlated with the event plane  $\Psi_2$  found using energy deposited in a region of the HF spanning  $-5 < \eta < -3$  ( $3 < \eta < 5$ ). This is chosen to introduce a rapidity gap between the particles used in the event plane determination and the  $J/\psi$  meson, in order to reduce the effect of other correlations that might exist, such as those from dijet production. To account for nonuniformities in the detector acceptance that can lead to artificial asymmetries in the event plane angle distribution and thereby affect the deduced  $v_2$  values, a Fourier analysis “flattening” procedure [59] is used, where each calculated event plane angle is shifted slightly to recover a uniform azimuthal distribution, as described in Ref. [58]. The event plane has a resolution that depends on centrality, and is caused by the finite number of particles used in its determination.

The corrections applied event-by-event ensure that the prompt and nonprompt yields extracted from fitting the invariant mass and  $\ell_{J/\psi}$  distributions account for reconstruction and selection inefficiencies. As such, after extracting the yields in each  $|y|$ ,  $p_T$ , centrality (and  $|\Delta\phi|$ ) bin, the  $v_2$  and  $R_{AA}$  can be calculated directly. The  $R_{AA}$  is defined by

$$R_{AA} = \frac{N_{PbPb}^{J/\psi}}{(T_{AA} \sigma_{pp}^{J/\psi})}, \tag{3}$$

where  $N_{PbPb}^{J/\psi}$  is the number of prompt or nonprompt  $J/\psi$  mesons produced per PbPb collision,  $\sigma_{pp}^{J/\psi}$  is the corresponding pp cross section, and  $T_{AA}$  is the nuclear overlap function.

The  $v_2$  is calculated by fitting the  $[1/N_{total}^{J/\psi}][dN^{J/\psi}/d|\Delta\phi|]$  distributions with the function  $1 + 2v_2^{obs} \cos(|2\Delta\phi|)$ , where the  $N_{total}^{J/\psi}$  is the prompt or nonprompt  $J/\psi$  yield integrated over azimuth for each kinematic bin. An example of such a fit is shown in Fig. 2. The final  $v_2$  coefficient in the event plane method is evaluated by dividing the observed

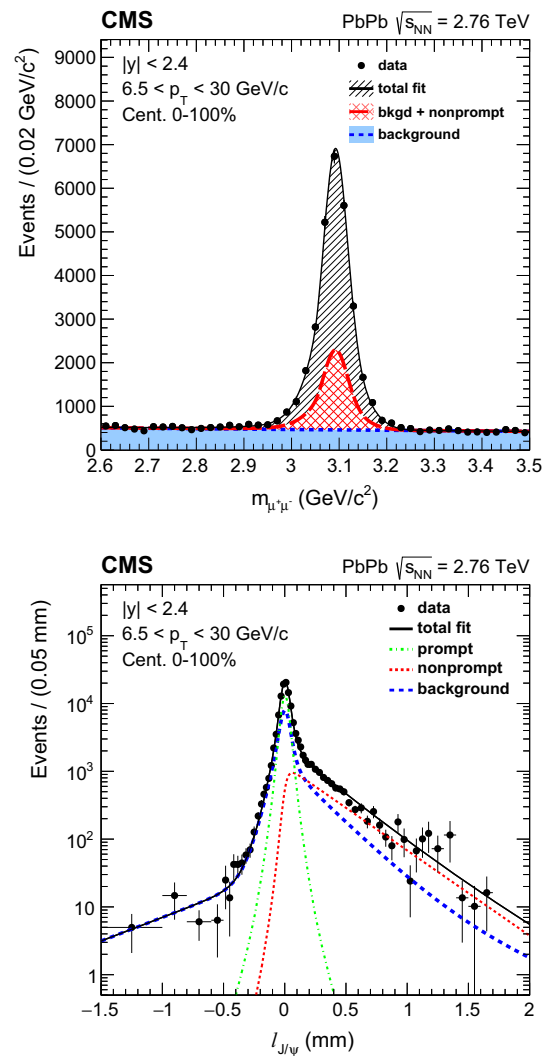


**Fig. 1** Invariant mass spectra (*top*) and pseudo-proper decay length distribution (*bottom*) of  $\mu^+\mu^-$  pairs in centrality 0–100% and integrated over the rapidity range  $|y| < 2.4$  and the  $p_T$  range  $6.5 < p_T < 30$  GeV/c. The *error bars* on each point represent statistical uncertainties. The projections of the two-dimensional fit onto the respective axes are overlaid as *solid black lines*. The *dashed green and red lines* show the fitted contribution of prompt and nonprompt  $J/\psi$ . The fitted background contributions are shown as *dotted blue lines*

value  $v_2^{obs}$  by an event-averaged resolution-correction  $R$ , i.e.  $v_2 = v_2^{obs}/R$ , as described in Ref. [60]. The factor  $R$ , calculated experimentally as described in Ref. [58], can range from 0 to 1, with a better resolution corresponding to a larger value of  $R$ . No difference is observed when determining  $R$  using the dimuon-triggered events analysed here, compared to the values used in Ref. [58] for the analysis of charged hadrons. For this paper, the  $v_2$  analysis is restricted to the centrality interval 10–60% to ensure a nonsymmetric overlap region in the colliding nuclei, while maintaining a good event plane resolution ( $R \gtrsim 0.8$  in the event centrality ranges

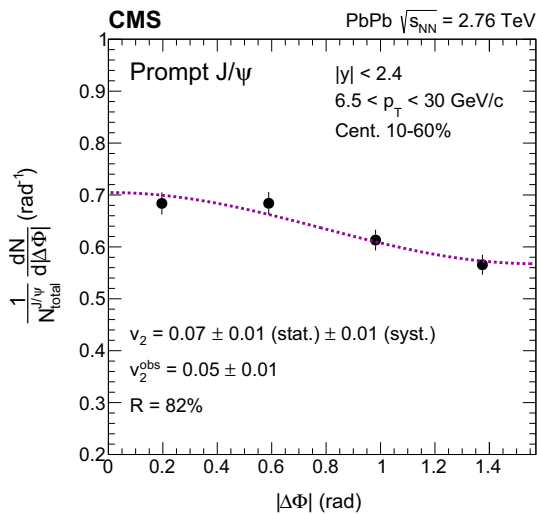


**Fig. 2** The  $|\Delta\Phi|$  distribution of high  $p_T$  prompt  $J/\psi$  mesons,  $6.5 < p_T < 30 \text{ GeV}/c$ , measured in the rapidity range  $|y| < 2.4$  and event centrality 10–60%, normalized by the bin width and the sum of the prompt yields in all four  $\Delta\Phi$  bins. The *dashed line* represents the function  $1 + 2v_2^{\text{obs}} \cos(2\Delta\Phi)$  used to extract the  $v_2^{\text{obs}}$ . The event-averaged resolution correction factor, corresponding to this event centrality, is also listed, together with the calculated final  $v_2$  for this kinematic bin. The systematic uncertainty listed in the legend includes the 2.7% global uncertainty from the event plane measurement

in which results are reported: 10–20%, 20–30%, and 30–60%).

### 3.3 Estimation of uncertainties

Several sources of systematic uncertainties are considered for both  $R_{AA}$  and  $v_2$  analyses. They are mostly common, thus calculated and propagated in a similar way.

The systematic uncertainties in the signal extraction method (fitting) are evaluated by varying the analytical form of each component of the PDF hypotheses. For the invariant mass PDF, as an alternative signal shape, a sum of two Gaussian functions is used, with shared mean and both widths as free parameters in the fit. For the same PDF, the uncertainty in the background shape is evaluated using a first order Chebyshev polynomial. For the differential centrality bins, with the invariant mass signal PDF parameters fixed to the 0–100% bin, an uncertainty is calculated by performing fits in which the constrained parameters are allowed to vary with a Gaussian PDF. The mean of the constraining Gaussian function and the initial value of the constrained parameters come from the fitting in the 0–100% bin with no fixed parameters. The uncertainties of the parameters in the 0–100% bin is used as a width of the constraining Gaussian. For the lifetime PDF components, the settings that could potentially affect the b fraction are changed. The  $\ell_{J/\psi}$  shape of the nonprompt  $J/\psi$  is taken directly from the reconstructed one in simulation and converted to a PDF. Tails of this PDF, where the MC statistics are insufficient, are mirrored from neighbor-

ing points, weighted with the corresponding efficiency. The sum in quadrature of all yield variations with respect to the nominal fit is propagated in the calculation of the systematic uncertainty in the final results. The variations across all  $R_{AA}$  ( $v_2$ ) analysis bins are between 0.7 and 16% (2.6 and 38%) for prompt  $J/\psi$ , and 1.4 and 19% (20 and 81%) for nonprompt  $J/\psi$ . They increase from mid to forward rapidity, from high- to low- $p_T$ , and for PbPb results also from central to peripheral bins.

Three independent uncertainties are assigned for the dimuon efficiency corrections. One addresses the uncertainty on the parametrization of the efficiency vs.  $p_T$ ,  $y$ , and centrality. For the  $R_{AA}$  results, it is estimated, in each signal  $y$  and centrality bin, by randomly moving 100 times, each individual efficiency versus  $p_T$  point within its statistical uncertainty, re-fitting with the Gaussian error function, and recalculating each time a corrected MC signal yield. For the  $v_2$  results, this procedure is not practical: it requires re-weighting and re-fitting many times the full data sample. So in this case, the uncertainty is estimated by changing two settings in the nominal efficiency, and re-fitting data only once, with the modified efficiency: (a) using binned efficiency instead of fits, and (b) using only the nonprompt  $J/\psi$  MC sample, integrated over all event centralities. The relative uncertainties for this source, propagated into the final results, are calculated for  $R_{AA}$  as the root-mean-square of the 100 yield variations with respect to the yield obtained with the nominal efficiency parametrization, and for the  $v_2$  analysis as the full difference between the nominal and the modified-efficiency results. Across all  $R_{AA}$  ( $v_2$ ) analysis bins, the values are between 0.6 and 20% (1.5 and 54%) for prompt  $J/\psi$ , and 0.7 and 24% (6.1 and 50%) for nonprompt  $J/\psi$  results. These uncertainties increase from high to low  $p_T$ , and from mid to forward rapidity but do not have a strong centrality dependence.

A second uncertainty addresses the accuracy of the efficiency vs.  $L_{xyz}$  calculation, and is estimated by changing the  $L_{xyz}$  resolution. It is done in several steps: (a) the binning in the  $L_{xyz}^{\text{true}}$  vs.  $L_{xyz}$  maps is changed; (b) the dimuon efficiency weights are recalculated; c) the data is reweighed and refitted to extract the signal yields. The variations across all  $R_{AA}$  ( $v_2$ ) analysis bins are between 0.025 and 3.7% (0.1 and 16%) for prompt  $J/\psi$ , and 0.1 and 13% (29 and 32%) for nonprompt  $J/\psi$  results. In the case of the prompt  $J/\psi$ , the variations are small and rather constant across all bins, around 2–3%, with the 16% variation being reached only in the lowest- $p_T$  bin in the  $v_2$  analysis. For nonprompt  $J/\psi$  the variations increase from mid to forward rapidity, and for PbPb also from peripheral to central bins.

Finally, a third class of uncertainty arises from the scaling factors. For the  $v_2$  analysis, the full difference between results with and without T&P corrections is propagated to the final systematic uncertainty. It varies between 0.4 and

7.4% for prompt  $J/\psi$ , and 5.4 and 8.8% for nonprompt  $J/\psi$  results. For the  $R_{AA}$  analysis, this uncertainty comprises two contributions. A parametrization uncertainty was estimated by randomly moving each of the data T&P efficiency points within their statistical uncertainty, recalculating each time the scaling factors and the dimuon efficiencies in all the analysis bins, and propagating the root-mean-square of all variations to the total T&P uncertainty. In addition, a systematic uncertainty was estimated by changing different settings of the T&P method. The contributions are similar for the prompt and nonprompt  $J/\psi$  results, and vary between 1.4 and 13% across all bins, for the combined trigger, identification, and reconstruction efficiencies, with the largest uncertainties in the forward and low  $p_T$  regions. On top of these bin-by-bin T&P uncertainties, an uncertainty in the tracking reconstruction efficiency, 0.3 and 0.6% for each muon track, for pp and PbPb, respectively, is doubled for dimuon candidates, and considered as a global uncertainty in the final results.

There is one additional source of uncertainty that is particular to each analysis. For the  $R_{AA}$  results, it is the  $T_{AA}$  uncertainty, which varies between 16 and 4.1% from most peripheral (70–100%) to most central (0–5%) events, and it has a value of 5.6% for the 0–100% case, estimated as described in Ref. [36]. For the  $v_2$  analysis, uncertainties are assigned for the event plane measurement. A systematic uncertainty is associated with the event plane flattening procedure and the resolution correction determination ( $\pm 1\%$  [60]), and another with the sensitivity of the measured  $v_2$  values to the size of the minimum  $\eta$  gap (2.5%, following Ref. [60]). The two uncertainties are added quadratically to a total of 2.7% global uncertainty in the  $v_2$  measurement.

The total systematic uncertainty in the  $R_{AA}$  is estimated by summing in quadrature the uncertainties from the signal extraction and efficiency weighting. The range of the final uncertainties on prompt and nonprompt  $J/\psi$   $R_{AA}$  is between 2.1 and 22%, and 2.8 and 28%, respectively, across bins of the analysis. The uncertainty in the integrated luminosity of the pp data (3.7%),  $N_{MB}$  events in PbPb data (3%), and tracking efficiency (0.6% for pp and 1.2% for PbPb data) are considered as global uncertainties.

The total systematic uncertainty for  $v_2$  is estimated by summing in quadrature the contributions from the yield extraction and efficiency corrections. The range of the final uncertainties on prompt and nonprompt  $J/\psi$   $v_2$  results is between 10 and 57%, and 37 and 100%, respectively.

### 3.4 Displaying uncertainties

In all the results shown, statistical uncertainties are represented by error bars, and systematic uncertainties by boxes centered on the points. For the  $v_2$  results, the global uncertainty from the event plane measurement is not included in the point-by-point uncertainties. Boxes plotted at  $R_{AA} = 1$  rep-

resent the scale of the global uncertainties. For  $R_{AA}$  results plotted as a function of  $p_T$  or  $|y|$ , the statistical and systematic uncertainties include the statistical and systematic components from both PbPb and pp samples, added in quadrature. For these types of results, the systematic uncertainty on  $T_{AA}$ , the pp sample integrated luminosity uncertainty, the uncertainty in the  $N_{MB}$  of PbPb events, and the tracking efficiency are added in quadrature and shown as a global uncertainty.

For  $R_{AA}$  results shown as a function of  $N_{part}$ , the uncertainties on  $T_{AA}$  are included in the systematic uncertainty, point-by-point. The global uncertainty plotted at  $R_{AA} = 1$  as a grey box includes in this case the statistical and systematic uncertainties from the pp measurement, the integrated luminosity uncertainty for the pp data, the uncertainty in the  $N_{MB}$  of PbPb events, and the tracking efficiency uncertainty, added in quadrature. When showing  $R_{AA}$  vs.  $N_{part}$  separately for different  $p_T$  or  $|y|$  intervals, the statistical and systematic uncertainties from the pp measurement are added together in quadrature and plotted as a coloured box at  $R_{AA} = 1$ . In addition, a second global uncertainty, that is common for all the  $p_T$  and  $|y|$  bins, is calculated as the quadratic sum of the integrated luminosity uncertainty for pp data, the uncertainty in  $N_{MB}$  of PbPb events, and the tracking efficiency uncertainty, and is plotted as an empty box at  $R_{AA} = 1$ .

## 4 Results

For all results plotted versus  $p_T$  or  $|y|$ , the abscissae of the points correspond to the centre of the respective bin, and the horizontal error bars reflect the width of the bin. When plotted as a function of centrality, the abscissae are average  $N_{part}$  values corresponding to events flatly distributed across centrality. For the  $R_{AA}$  results, the numerical values of the numerator and denominator of Eq. (3) are available in tabulated form in Appendix A.

### 4.1 Prompt $J/\psi$

The measured prompt  $J/\psi$   $v_2$ , for 10–60% event centrality and integrated over  $6.5 < p_T < 30$  GeV/c and  $|y| < 2.4$ , is  $0.066 \pm 0.014$  (stat)  $\pm 0.014$  (syst)  $\pm 0.002$  (global). The significance corresponding to a deviation from a  $v_2 = 0$  value is 3.3 sigma. Figure 3 shows the dependence of  $v_2$  on centrality,  $|y|$ , and  $p_T$ . For each of these results, the dependence on one variable is studied by integrating over the other two. A nonzero  $v_2$  value is measured in all the kinematic bins studied. The observed anisotropy shows no strong centrality, rapidity, or  $p_T$  dependence.

In Fig. 4, the  $R_{AA}$  of prompt  $J/\psi$  as a function of centrality,  $|y|$ , and  $p_T$  are shown, integrating in each case over the other two variables. The  $R_{AA}$  is suppressed even for the most peripheral bin (60–100%), with the suppression slowly

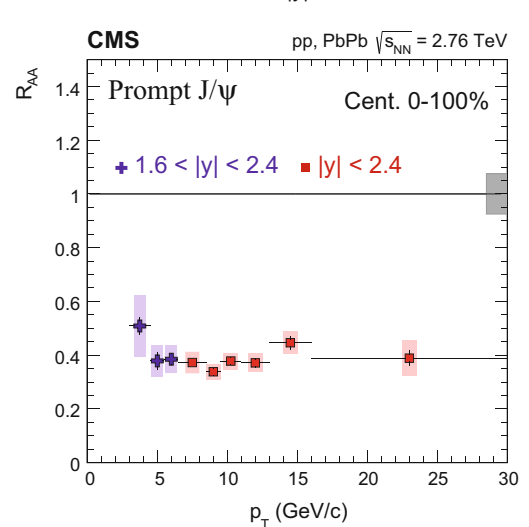
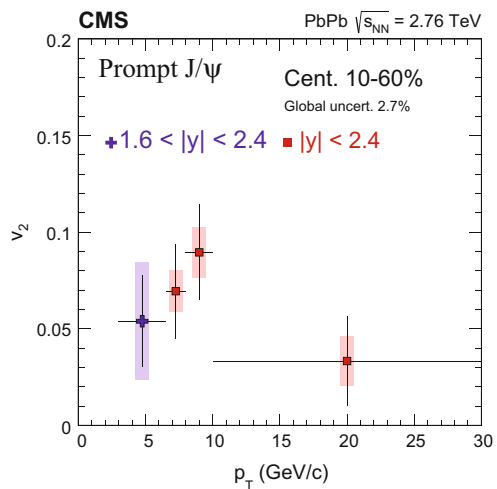
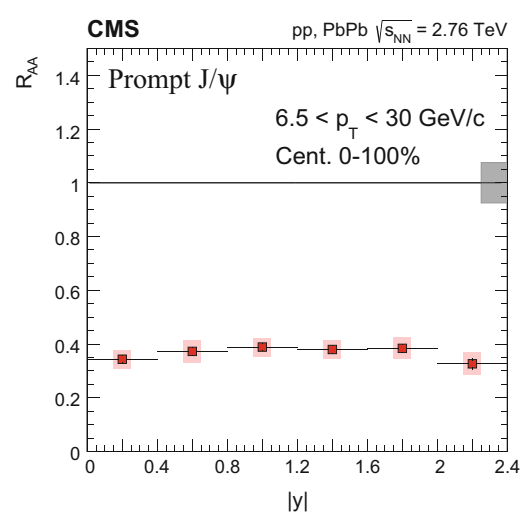
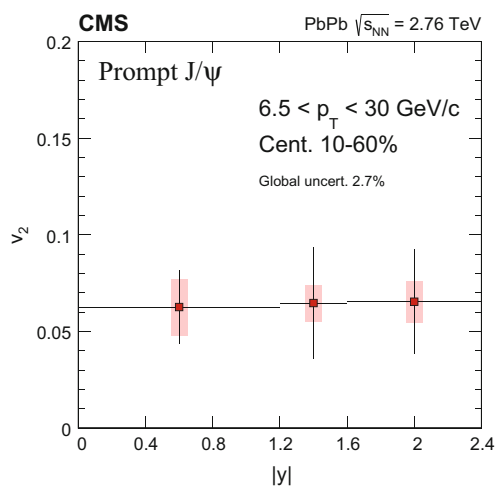
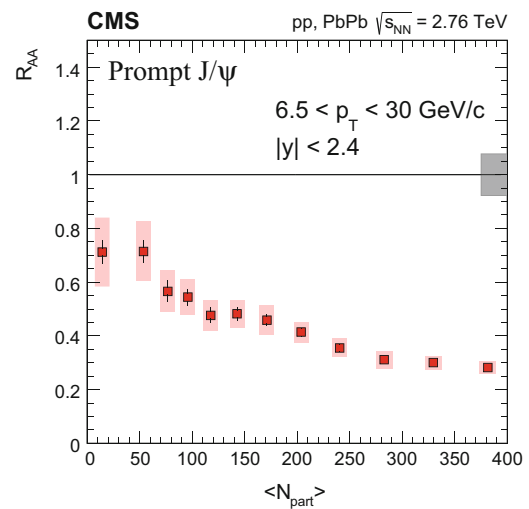
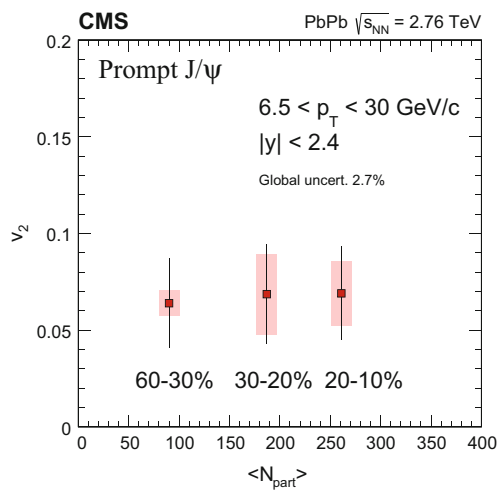


**Fig. 3** Prompt J/ $\psi$   $v_2$  as a function of centrality (top), rapidity (middle), and  $p_T$  (bottom). The bars (boxes) represent statistical (systematic) point-by-point uncertainties. The global uncertainty, listed in the legend, is not included in the point-by-point uncertainties. Horizontal bars indicate the bin width. The average  $N_{part}$  values correspond to events flatly distributed across centrality

**Fig. 4** Prompt J/ $\psi$   $R_{AA}$  as a function of centrality (top), rapidity (middle), and  $p_T$  (bottom). The bars (boxes) represent statistical (systematic) point-by-point uncertainties. The gray boxes plotted on the right side at  $R_{AA} = 1$  represent the scale of the global uncertainties. The average  $N_{part}$  values correspond to events flatly distributed across centrality



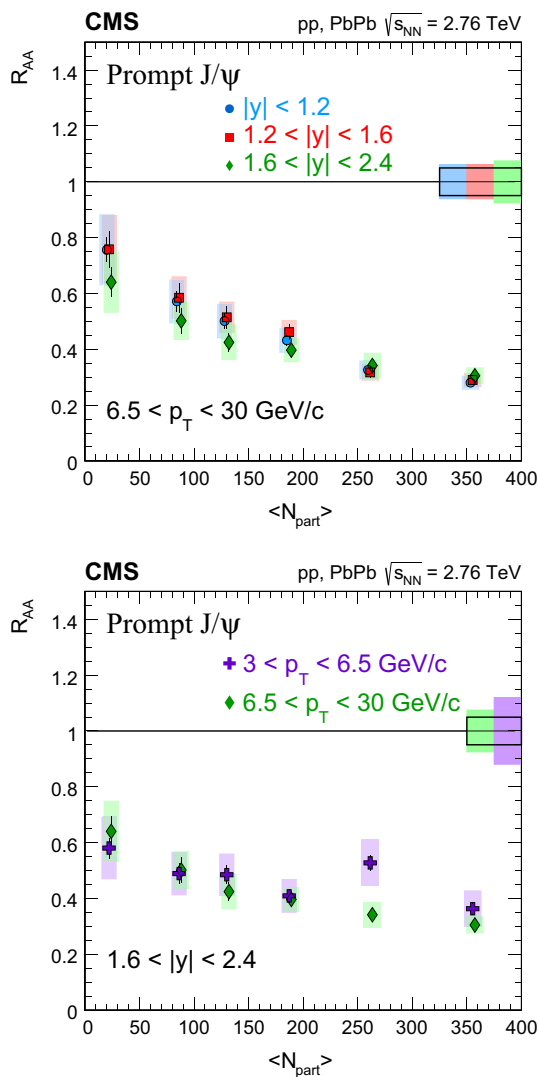


**Fig. 5** *Top* Prompt J/ψ  $R_{AA}$  as a function of centrality at high  $p_T$ ,  $6.5 < p_T < 30$  GeV/c, for three different  $|y|$  regions. The high- $p_T$  mid- and forward-rapidity points are shifted horizontally by  $\Delta N_{part} = 2$  for better visibility. *Bottom* Prompt J/ψ  $R_{AA}$  as a function of centrality, at forward rapidity,  $1.6 < |y| < 2.4$ , for two different  $p_T$  regions. The bars (boxes) represent statistical (systematic) point-by-point uncertainties. The boxes plotted on the right side at  $R_{AA} = 1$  represent the scale of the global uncertainties: the coloured boxes show the statistical and systematic uncertainties from pp measurement, and the open box shows the global uncertainties common to all data points. The average  $N_{part}$  values correspond to events flatly distributed across centrality

increasing with  $N_{part}$ . The  $R_{AA}$  for the most central events (0–5%) is measured for  $6.5 < p_T < 30$  GeV/c and  $|y| < 2.4$  to be  $0.282 \pm 0.010$  (stat)  $\pm 0.023$  (syst). No strong rapidity or  $p_T$  dependence of the suppression is observed.

Two double-differential studies are also made, in which a simultaneous binning in centrality and  $|y|$ , or in centrality and  $p_T$  is done. Figure 5 (top) shows the centrality dependence of high  $p_T$  ( $6.5 < p_T < 30$  GeV/c) prompt J/ψ  $R_{AA}$  measured in three  $|y|$  intervals. A similar suppression pattern is observed for all rapidities. Figure 5 (bottom) shows,

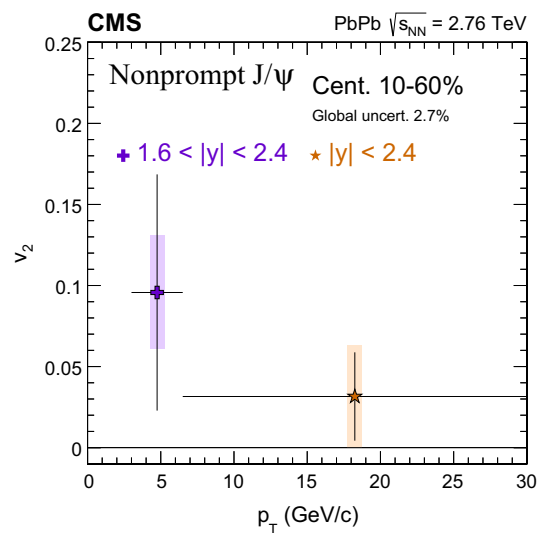


**Fig. 6** Nonprompt J/ψ  $v_2$  as a function of  $p_T$ . The bars (boxes) represent statistical (systematic) point-by-point uncertainties. The global uncertainty, listed in the legend, is not included in the point-by-point uncertainties. Horizontal bars indicate the bin width

for  $1.6 < |y| < 2.4$ , the  $p_T$  dependence of  $R_{AA}$  vs.  $N_{part}$ . The suppression at low  $p_T$  ( $3 < p_T < 6.5$  GeV/c) is consistent with that at high  $p_T$  ( $6.5 < p_T < 30$  GeV/c).

#### 4.2 Nonprompt J/ψ

Figure 6 shows the nonprompt J/ψ  $v_2$  vs.  $p_T$  for 10–60% event centrality, in two kinematic regions:  $6.5 < p_T < 30$  GeV/c and  $|y| < 2.4$ , and  $3 < p_T < 6.5$  GeV/c and  $1.6 < |y| < 2.4$ . The measured  $v_2$  for the high-(low-)  $p_T$  is  $0.032 \pm 0.027$  (stat)  $\pm 0.032$  (syst)  $\pm 0.001$  (global) ( $0.096 \pm 0.073$  (stat)  $\pm 0.035$  (syst)  $\pm 0.003$  (global)). This is obtained from the fit to the  $|\Delta\Phi|$  distribution (as described in Sect. 3.2) with a  $\chi^2$  probability of 22(20)%. Fitting the same distribution with a constant (corresponding to the  $v_2 = 0$  case) the  $\chi^2$  probability is 11(8)%. Both measurements are consistent with each other and with a  $v_2$  value of zero, though both nominal values are positive.

In Fig. 7, the  $R_{AA}$  of nonprompt J/ψ as a function of centrality,  $|y|$ , and  $p_T$  are shown, integrating in each case over the other two variables. A steady increase of the suppression is observed with increasing centrality of the collision. The  $R_{AA}$  for the most central events (0–10%) measured for  $6.5 < p_T < 30$  GeV/c and  $|y| < 2.4$  is  $0.332 \pm 0.017$  (stat)  $\pm 0.028$  (syst). Stronger suppression is observed with both increasing rapidity and  $p_T$ .

As for the prompt production case, two double-differential studies were done, simultaneously binning in centrality and  $|y|$  or  $p_T$ . Figure 8 (top) shows the rapidity dependence of  $R_{AA}$  vs.  $N_{part}$  for high  $p_T$  nonprompt J/ψ. Figure 8 (bottom) shows, for  $1.6 < |y| < 2.4$ , the  $p_T$  dependence of  $R_{AA}$  vs.  $N_{part}$ . The centrality dependences of the three  $|y|$  intervals

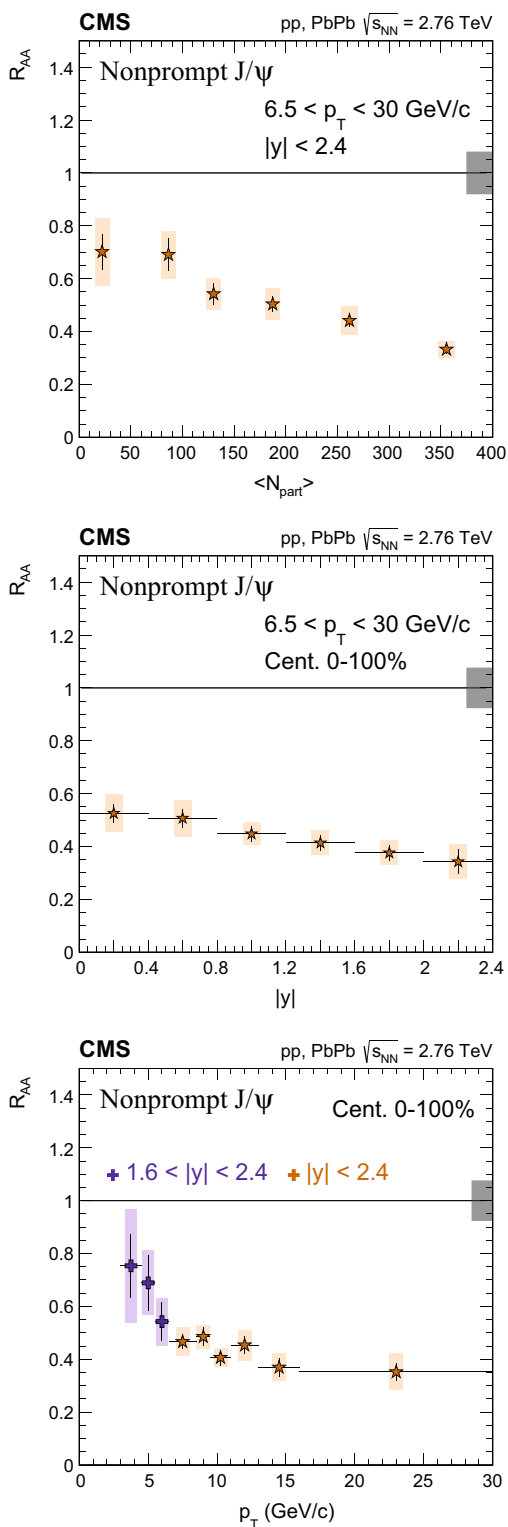


**Fig. 7** Nonprompt  $J/\psi$   $R_{AA}$  as a function of centrality (*top*), rapidity (*middle*), and  $p_T$  (*bottom*). The *bars (boxes)* represent statistical (systematic) point-by-point uncertainties. The *gray boxes* plotted on the right side at  $R_{AA} = 1$  represent the scale of the global uncertainties. For  $R_{AA}$  vs.  $N_{part}$ , the average  $N_{part}$  values correspond to events flatly distributed across centrality

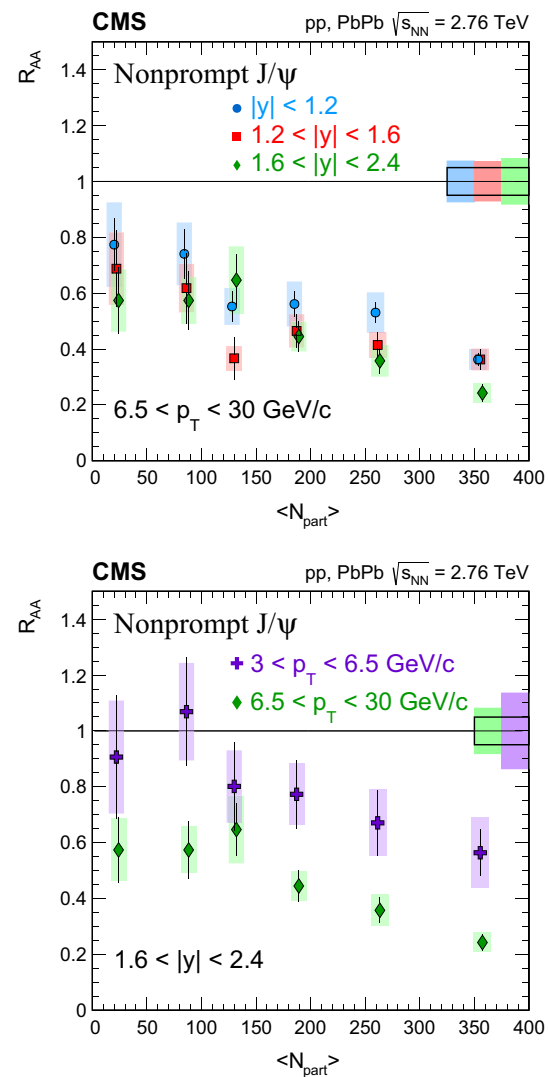


**Fig. 8** *Top* Nonprompt  $J/\psi$   $R_{AA}$  as a function of centrality at high  $p_T$ ,  $6.5 < p_T < 30 \text{ GeV}/c$ , for three different  $|y|$  regions. The high- $p_T$  mid- and forward-rapidity points are shifted horizontally by  $\Delta N_{part} = 2$  for better visibility. *Bottom* Nonprompt  $J/\psi$   $R_{AA}$  as a function of centrality, at forward rapidity,  $1.6 < |y| < 2.4$ , for two different  $p_T$  regions. The *bars (boxes)* represent statistical (systematic) point-by-point uncertainties. The *boxes* plotted on the right side at  $R_{AA} = 1$  represent the scale of the global uncertainties: the *coloured boxes* show the statistical and systematic uncertainties from pp measurement, and the *open box* shows the global uncertainties common to all data points. The average  $N_{part}$  values correspond to events flatly distributed across centrality

are quite similar, and the same is true for the two  $p_T$  ranges. As was also seen in Fig. 7, smaller suppression is observed at lower  $|y|$  and lower  $p_T$ .

## 5 Discussion

In this section, the  $R_{AA}$  and  $v_2$  results are compared first for open and hidden charm, and then for open charm and

beauty, using data from the ALICE experiment [31,61,62]. For open charm, the measurements of  $R_{AA}$  vs.  $N_{part}$  of prompt  $D^0$  mesons, and of averaged prompt D mesons ( $D^0$ ,  $D^+$  and  $D^{*+}$  combined), measured in  $|y| < 0.5$  at low  $p_T$  ( $2 < p_T < 5$  GeV/c), and high  $p_T$  ( $6 < p_T < 12$  GeV/c) [61] are used. These are compared to hidden charm data from the prompt  $J/\psi$  results described in this paper, in two  $p_T$  regions that are similar to the D measurement, i.e. ( $3 < p_T < 6.5$  GeV/c,  $1.6 < |y| < 2.4$ ) and ( $6.5 < p_T < 30$  GeV/c,  $|y| < 1.2$ ). For the  $R_{AA}$  comparison of open charm vs. beauty, the averaged prompt D mesons measured in  $|y| < 0.5$  [62] are compared to the nonprompt  $J/\psi$  results reported in this paper for  $|y| < 1.2$ . The  $p_T$  interval ( $8 < p_T < 16$  GeV/c) for the D is chosen to correspond to that of the parent B mesons of the CMS nonprompt  $J/\psi$  result [62].

For the  $v_2$  results, the  $p_T$  dependence reported in this paper for both prompt and nonprompt  $J/\psi$  in the centrality 10–60% bin are compared with the  $v_2$  of the averaged D mesons [31] measured in the 30–50% centrality bin. In addition, the CMS charged-hadron  $v_2$  results, measured for  $|\eta| < 0.5$ , derived for 10–60% centrality bin from Refs. [60] and [58], are added to the comparison.

### 5.1 Open versus hidden charm

The top two panels of Fig. 9 show the  $R_{AA}$  dependence on the centrality of the prompt  $J/\psi$  (bound  $Q\bar{Q}$  state) and of prompt D (charm-light states  $Q\bar{q}$ ) mesons, for low- (*top*) and high- (*middle*)  $p_T$  selections. In both cases, the mesons suffer a similar suppression, over the whole  $N_{part}$  range, even though the charmonium yield should be affected by colour screening [4,48], potentially by final-state nuclear interactions unrelated to the QGP [63–67], and by rather large feed-down contributions from excited states [68,69]. Moreover, common processes (i.e. recombination or energy loss effects) are expected to affect differently the open and hidden charm [26,27,70,71]. While the present results cannot resolve all these effects, the comparison of open and hidden charm could help to determine their admixture.

A comparison of the  $p_T$  dependence of the azimuthal anisotropy  $v_2$  between the prompt  $J/\psi$  and D mesons is made in the bottom panel of Fig. 9. While the  $R_{AA}$  is similar both at low and high  $p_T$ , the  $v_2$  of prompt  $J/\psi$  at low  $p_T$  is lower than that of both D mesons and charged hadrons. At high  $p_T$ , all three results, within the uncertainties, are similar: the prompt  $J/\psi$  results seem to point to a similar anisotropy as the light-quarks hadrons, hinting at a flavour independence of the energy-loss path-length dependence. The prompt  $J/\psi$  results could help advance the theoretical knowledge on the relative contribution of the regenerated charmonium yield, as this is the only type of  $J/\psi$  expected to be affected by the collective expansion of the medium. Such prompt  $J/\psi$

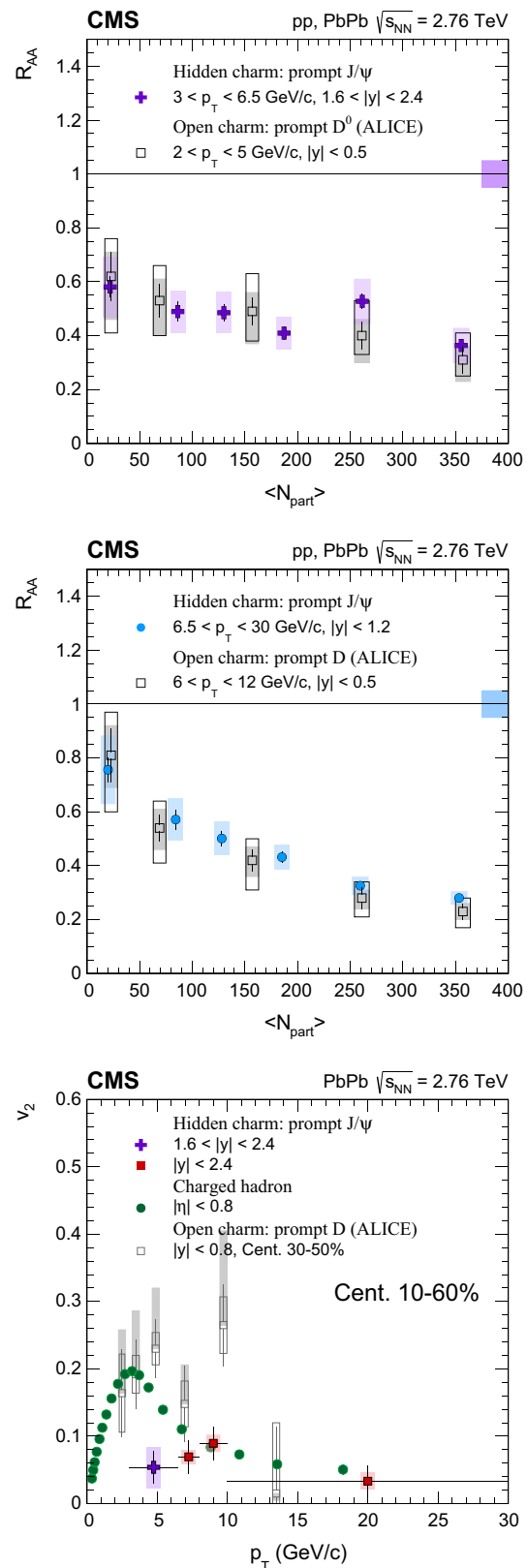


**Fig. 9** Prompt  $J/\psi$  and D meson [61]  $R_{AA}$  vs. centrality for low  $p_T$  (*top*) and high  $p_T$  (*middle*). The average  $N_{part}$  values correspond to events flatly distributed across centrality. *Bottom* Prompt  $J/\psi$  and D meson [31], and charged hadron [58,60]  $v_2$  vs.  $p_T$

should have higher  $v_2$  values, closer to those of light-quark hadrons [27].

## 5.2 Open charm versus beauty

The *top* panel of Fig. 10 shows the  $R_{AA}$  dependence on centrality of the nonprompt  $J/\psi$  (decay product of B mesons originating from b quarks) and for D mesons (originating from c quarks). The D mesons are more suppressed than the nonprompt  $J/\psi$ . This is expected in models that assume less radiative energy loss for the b quark compared to that of a c quark because of the ‘dead-cone effect’ (the suppression of gluon bremsstrahlung of a quark with mass  $m$  and energy  $E$ , for angles  $\theta < m/E$  [72,73]), and smaller collisional energy loss for the much heavier b quark than for the c quark [15,74]. The results bring extra information in a kinematic phase space not accessible with fully reconstructed b jet measurements, which show that for  $p_T > 80$  GeV/c the  $R_{AA}$  of b jets is compatible to that of light-quark or gluon jets [75]. However, assessing and quantifying the parton mass dependence of the in-medium phenomena is not trivial: one has to account among other things for different starting kinematics (different unmodified vacuum spectra of the beauty and charm quarks in the medium), and the effect of different fragmentation functions (and extra decay kinematics) [76]. Also, when considering the parton mass dependence, it should be noted that at high- $p_T$ , the  $R_{AA}$  of D mesons was found to be similar to that of charged pions over a wide range of event centrality [31].

The *bottom* panel of Fig. 10 shows the  $p_T$  dependence of the measured  $v_2$  for nonprompt  $J/\psi$ , prompt D mesons, and charged hadrons. The precision and statistical reach of the present LHC open beauty and charm  $v_2$  results can not answer: (a) at low  $p_T$ , whether the b quarks, with their mass much larger than that of the charm quarks, participate or not in the collective expansion of the medium as the charm quarks seem to do; (b) at high  $p_T$ , whether there is a difference in path-length dependence of energy loss between b and c quarks.

## 6 Summary

The production of prompt and nonprompt (coming from b hadron decay)  $J/\psi$  has been studied in pp and PbPb collisions at  $\sqrt{s_{NN}} = 2.76$  TeV. The  $R_{AA}$  of the prompt  $J/\psi$  mesons, integrated over the rapidity range  $|y| < 2.4$  and high  $p_T$ ,  $6.5 < p_T < 30$  GeV/c, is measured in 12 centrality bins. The  $R_{AA}$  is less than unity even in the most peripheral bin, and the suppression becomes steadily stronger as centrality increases. Integrated over rapidity ( $p_T$ ) and centrality, no strong evidence for a  $p_T$  (rapidity) dependence of the suppression is found. The azimuthal anisotropy of prompt  $J/\psi$

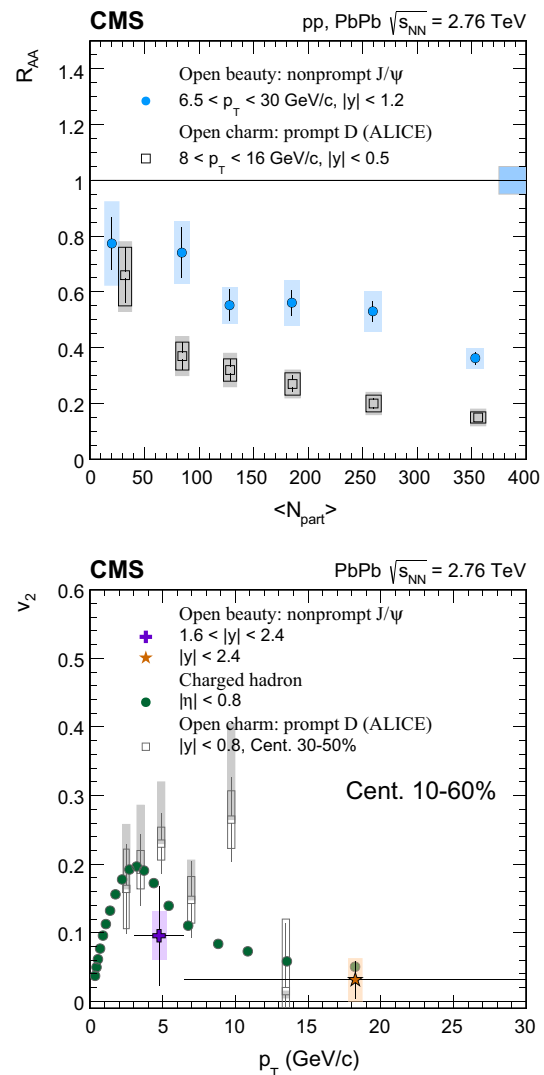


**Fig. 10** Nonprompt  $J/\psi$  and prompt D meson [31,62], and charged hadron [58,60]  $R_{AA}$  vs. centrality (*top*), and  $v_2$  vs.  $p_T$  (*bottom*). For the *top* plot, the average  $N_{part}$  values correspond to events flatly distributed across centrality

mesons shows a nonzero  $v_2$  value in all studied bins, while no strong dependence on centrality, rapidity, or  $p_T$  is observed.

The  $R_{AA}$  of nonprompt  $J/\psi$  mesons shows a slow decrease with increasing centrality and rapidity. The results show less suppression at low  $p_T$ . The first measurement of the nonprompt  $J/\psi$   $v_2$  is also reported in two  $p_T$  bins for 10–60% event centrality, and the values are consistent with zero elliptical azimuthal anisotropy, though both nominal values are positive.

**Acknowledgements** We congratulate our colleagues in the CERN accelerator departments for the excellent performance of the LHC and thank the technical and administrative staffs at CERN and at other CMS institutes for their contributions to the success of the CMS effort. In addition, we gratefully acknowledge the computing centres and personnel of the Worldwide LHC Computing Grid for delivering so effec-



tively the computing infrastructure essential to our analyses. Finally, we acknowledge the enduring support for the construction and operation of the LHC and the CMS detector provided by the following funding agencies: the Austrian Federal Ministry of Science, Research and Economy and the Austrian Science Fund; the Belgian Fonds de la Recherche Scientifique, and Fonds voor Wetenschappelijk Onderzoek; the Brazilian Funding Agencies (CNPq, CAPES, FAPERJ, and FAPESP); the Bulgarian Ministry of Education and Science; CERN; the Chinese Academy of Sciences, Ministry of Science and Technology, and National Natural Science Foundation of China; the Colombian Funding Agency (COLCIENCIAS); the Croatian Ministry of Science, Education and Sport, and the Croatian Science Foundation; the Research Promotion Foundation, Cyprus; the Secretariat for Higher Education, Science, Technology and Innovation, Ecuador; the Ministry of Education and Research, Estonian Research Council via IUT23-4 and IUT23-6 and European Regional Development Fund, Estonia; the Academy of Finland, Finnish Ministry of Education and Culture, and Helsinki Institute of Physics; the Institut National de Physique Nucléaire et de Physique des Particules / CNRS, and Commissariat à l'Énergie Atomique et aux Énergies Alternatives / CEA, France; the Bundesministerium für Bildung und Forschung, Deutsche Forschungsgemeinschaft, and Helmholtz-Gemeinschaft Deutscher Forschungszentren, Germany; the General Secretariat for Research and Technology, Greece; the National Scientific Research Foundation, and National Innovation Office, Hungary; the Department of Atomic Energy and the Department of Science and Technology, India; the Institute for Studies in Theoretical Physics and Mathematics, Iran; the Science Foundation, Ireland; the Istituto Nazionale di Fisica Nucleare, Italy; the Ministry of Science, ICT and Future Planning, and National Research Foundation (NRF), Republic of Korea; the Lithuanian Academy of Sciences; the Ministry of Education, and University of Malaya (Malaysia); the Mexican Funding Agencies (BUAP, CINVESTAV, CONACYT, LNS, SEP, and UASLP-FAI); the Ministry of Business, Innovation and Employment, New Zealand; the Pakistan Atomic Energy Commission; the Ministry of Science and Higher Education and the National Science Centre, Poland; the Fundação para a Ciência e a Tecnologia, Portugal; JINR, Dubna; the Ministry of Education and Science of the Russian Federation, the Federal Agency of Atomic Energy of the Russian Federation, Russian Academy of Sciences, and the Russian Foundation for Basic Research; the Ministry of Education, Science and Technological Development of Serbia; the Secretaría de Estado de Investigación, Desarrollo e Innovación and Programa Consolider-Ingenio 2010, Spain; the Swiss Funding Agencies (ETH Board, ETH Zurich, PSI, SNF, UniZH, Canton Zurich, and SER); the Ministry of Science and Technology, Taipei; the Thailand Center of Excellence in Physics, the Institute for the Promotion of Teaching Science and Technology of Thailand, Special Task Force for Activating Research and the National Science and Technology Development Agency of Thailand; the Scientific and Technical Research Council of Turkey, and Turkish Atomic Energy Authority; the National Academy of Sciences of Ukraine, and State Fund for Fundamental Researches, Ukraine; the Science and Technology Facilities Council, UK; the US Department of Energy, and the US National Science Foundation. Individuals have received support from the Marie-Curie programme and the European Research Council and EPLANET (European Union); the Leventis Foundation; the A. P. Sloan Foundation; the Alexander von Humboldt Founda-

tion; the Belgian Federal Science Policy Office; the Fonds pour la Formation à la Recherche dans l'Industrie et dans l'Agriculture (FRIA-Belgium); the Agentschap voor Innovatie door Wetenschap en Technologie (IWT-Belgium); the Ministry of Education, Youth and Sports (MEYS) of the Czech Republic; the Council of Science and Industrial Research, India; the HOMING PLUS programme of the Foundation for Polish Science, cofinanced from European Union, Regional Development Fund, the Mobility Plus programme of the Ministry of Science and Higher Education, the National Science Center (Poland), contracts Harmonia 2014/14/M/ST2/00428, Opus 2013/11/B/ST2/04202, 2014/13/B/ST2/02543 and 2014/15/B/ST2/03998, Sonata-bis 2012/07/E/ST2/01406; the Thalís and Aristeia programmes cofinanced by EU-ESF and the Greek NSRF; the National Priorities Research Program by Qatar National Research Fund; the Programa Clarín-COFUND del Principado de Asturias; the Rachadapisek Sompot Fund for Postdoctoral Fellowship, Chulalongkorn University and the Chulalongkorn Academic into Its 2nd Century Project Advancement Project (Thailand); and the Welch Foundation, contract C-1845.

**Open Access** This article is distributed under the terms of the Creative Commons Attribution 4.0 International License (<http://creativecommons.org/licenses/by/4.0/>), which permits unrestricted use, distribution, and reproduction in any medium, provided you give appropriate credit to the original author(s) and the source, provide a link to the Creative Commons license, and indicate if changes were made. Funded by SCOAP<sup>3</sup>.

## A Supplemental Material

The nominator and denominator of the  $R_{AA}$ , defined in Eq. (3), and presented in this paper in Figs. 4 and 5 for prompt  $J/\psi$ , and Figs. 7 and 8 for nonprompt  $J/\psi$ , are tabulated. They represent the efficiency-corrected signal yield within the single muon kinematic region used in this paper. This kinematic region is defined in Eq. (4). These  $\sqrt{s_{NN}} = 2.76$  TeV pp and PbPb fiducial cross sections do not depend on the acceptance, or the associated uncertainties. The corresponding  $T_{AA}$  values used in each case are also tabulated.

$$\begin{aligned} p_T^\mu &> 3.4 \text{ GeV}/c && \text{for } |\eta^\mu| < 1.0, \\ p_T^\mu &> (5.8 - 2.4 |\eta^\mu|) \text{ GeV}/c && \text{for } 1.0 < |\eta^\mu| < 1.5, \\ p_T^\mu &> (3.4 - 0.78 |\eta^\mu|) \text{ GeV}/c && \text{for } 1.5 < |\eta^\mu| < 2.4. \end{aligned} \quad (4)$$

### A.1 Prompt $J/\psi$

See Tables 1, 2, 3 and 4.

**Table 1** The prompt  $J/\psi$  fiducial cross section in bins of centrality, measured in PbPb and pp collisions at 2.76 TeV within the muon acceptance defined by Eq. (4), and the nuclear overlap function ( $T_{AA}$ , with its systematic uncertainty). Listed uncertainties are statistical first and sys-

tematic second. A global systematic uncertainty of 3.2% (3.7%) affects all PbPb (pp) fiducial cross sections. The table corresponds to the top panel of Fig. 4

Centrality (%)	$T_{AA}$ ( $\text{mb}^{-1}$ )	PbPb $\frac{1}{T_{AA}} \frac{d^3 N_{\text{PbPb}}^{J/\psi}}{dy d p_T d \text{Cent.}}$ (pb/GeV/c)	pp $\frac{d^2 \sigma_{\text{pp}}^{J/\psi}}{dy d p_T}$ (pb/GeV/c)
$ y  < 2.4, 6.5 < p_T < 30 \text{ GeV}/c$			
60–100	$0.246 \pm 0.041$	$50 \pm 3 \pm 9$	$69.6 \pm 0.6 \pm 4.1$
50–60	$1.36 \pm 0.19$	$50 \pm 3 \pm 8$	
45–50	$2.29 \pm 0.26$	$39 \pm 3 \pm 5$	
40–45	$3.20 \pm 0.34$	$38 \pm 2 \pm 5$	
35–40	$4.4 \pm 0.4$	$33 \pm 2 \pm 4$	
30–35	$5.8 \pm 0.5$	$34 \pm 2 \pm 4$	
25–30	$7.7 \pm 0.5$	$32 \pm 1 \pm 4$	
20–25	$9.9 \pm 0.6$	$29 \pm 1 \pm 3$	
15–20	$12.7 \pm 0.7$	$25 \pm 1 \pm 2$	
10–15	$16.2 \pm 0.8$	$21.7 \pm 0.9 \pm 2.3$	
5–10	$20.5 \pm 0.9$	$20.9 \pm 0.8 \pm 1.7$	
0–5	$25.9 \pm 1.1$	$19.6 \pm 0.7 \pm 1.6$	

**Table 2** The prompt  $J/\psi$  fiducial cross section in bins of absolute rapidity, measured in PbPb and pp collisions at 2.76 TeV within the muon acceptance defined by Eq. (4), and the nuclear overlap function ( $T_{AA}$ , with its systematic uncertainty). Listed uncertainties are statistical first

and systematic second. A global systematic uncertainty of 6.5% (3.7%) affects all PbPb (pp) fiducial cross sections. The table corresponds to the middle panel of Fig. 4

$ y $	$T_{AA}$ ( $\text{mb}^{-1}$ )	PbPb $\frac{1}{T_{AA}} \frac{d^2 N_{\text{PbPb}}^{J/\psi}}{dy d p_T}$ (pb/GeV/c)	pp $\frac{d^2 \sigma_{\text{pp}}^{J/\psi}}{dy d p_T}$ (pb/GeV/c)
Cent. 0–100%, $6.5 < p_T < 30 \text{ GeV}/c$			
0.0–0.4	$5.67 \pm 0.32$	$18.1 \pm 0.6 \pm 1.4$	$53 \pm 1 \pm 3$
0.4–0.8		$21.1 \pm 0.7 \pm 1.8$	$57 \pm 1 \pm 4$
0.8–1.2		$28.7 \pm 0.9 \pm 2.0$	$74 \pm 1 \pm 4$
1.2–1.6		$36 \pm 1 \pm 2$	$94 \pm 2 \pm 6$
1.6–2.0		$38 \pm 1 \pm 3$	$98 \pm 2 \pm 7$
2.0–2.4		$14.4 \pm 0.8 \pm 1.4$	$44 \pm 1 \pm 4$

**Table 3** The prompt  $J/\psi$  fiducial cross section in bins of  $p_T$ , measured in PbPb and pp collisions at 2.76 TeV within the muon acceptance defined by Eq. (4), and the nuclear overlap function ( $T_{AA}$ , with its systematic uncertainty). Listed uncertainties are statistical first and systematic second. A global systematic uncertainty of 6.5% (3.7%) affects all PbPb (pp) fiducial cross sections. The table corresponds to the bottom panel of Fig. 4

$p_T$ (GeV/c)	$T_{AA}$ ( $\text{mb}^{-1}$ )	PbPb $\frac{1}{T_{AA}} \frac{d^2 N_{\text{PbPb}}^{J/\psi}}{dy d p_T}$ (pb/GeV/c)	pp $\frac{d^2 \sigma_{\text{pp}}^{J/\psi}}{dy d p_T}$ (pb/GeV/c)
Cent. 0–100%, $1.6 <  y  < 2.4$			
3–4.5	$5.67 \pm 0.32$	$272 \pm 16 \pm 40$	$534 \pm 10 \pm 90$
4.5–5.5		$181 \pm 15 \pm 23$	$478 \pm 10 \pm 41$
5.5–6.5		$137 \pm 7 \pm 14$	$355 \pm 8 \pm 28$
Cent. 0–100%, $ y  < 2.4$			
6.5–8.5	$5.67 \pm 0.32$	$169 \pm 4 \pm 14$	$455 \pm 5 \pm 33$
8.5–9.5		$85 \pm 3 \pm 5$	$252 \pm 5 \pm 15$
9.5–11		$55 \pm 2 \pm 3$	$147 \pm 3 \pm 8$
11–13		$26 \pm 1 \pm 2$	$70 \pm 2 \pm 4$
13–16		$11.5 \pm 0.5 \pm 0.9$	$25.8 \pm 0.8 \pm 1.2$
16–30		$1.25 \pm 0.08 \pm 0.20$	$3.23 \pm 0.14 \pm 0.14$

**Table 4** The prompt  $J/\psi$  fiducial cross section in bins of centrality, for three  $|y|$  and two  $p_T$  intervals, measured in PbPb and pp collisions at 2.76 TeV within the muon acceptance defined by Eq. (4), and the nuclear overlap function ( $T_{AA}$ , with its systematic uncertainty). Listed uncertainties are statistical first and systematic second. A global systematic uncertainty of 3.2% (3.7%) affects all PbPb (pp) fiducial cross sections. The table corresponds to Fig. 5

Centrality (%)	$T_{AA}$ (mb <sup>-1</sup> )	PbPb $\frac{1}{T_{AA}} \frac{d^3 N_{J/\psi}^{PbPb}}{dy dp_T dCent.}$ (pb/GeV/c)	pp $\frac{d^2 \sigma_{pp}^{J/\psi}}{dy dp_T}$ (pb/GeV/c)
$0 <  y  < 1.2, 6.5 < p_T < 30$ GeV/c			
50–100	$0.468 \pm 0.070$	$47 \pm 3 \pm 8$	$61.4 \pm 0.7 \pm 3.7$
40–50	$2.75 \pm 0.30$	$35 \pm 2 \pm 5$	
30–40	$5.1 \pm 0.4$	$31 \pm 2 \pm 4$	
20–30	$8.8 \pm 0.6$	$27 \pm 1 \pm 3$	
10–20	$14.5 \pm 0.8$	$20.0 \pm 0.8 \pm 2.1$	
0–10	$23 \pm 1$	$17.2 \pm 0.7 \pm 1.6$	
$1.2 <  y  < 1.6, 6.5 < p_T < 30$ GeV/c			
50–100	$0.468 \pm 0.070$	$71 \pm 6 \pm 12$	$94 \pm 2 \pm 6$
40–50	$2.75 \pm 0.30$	$55 \pm 5 \pm 7$	
30–40	$5.1 \pm 0.4$	$48 \pm 4 \pm 5$	
20–30	$8.8 \pm 0.6$	$43 \pm 3 \pm 4$	
10–20	$14.5 \pm 0.8$	$30 \pm 2 \pm 3$	
0–10	$23 \pm 1$	$27 \pm 1 \pm 2$	
$1.6 <  y  < 2.4, 6.5 < p_T < 30$ GeV/c			
50–100	$0.468 \pm 0.070$	$46 \pm 4 \pm 8$	$71 \pm 1 \pm 5$
40–50	$2.75 \pm 0.30$	$36 \pm 3 \pm 5$	
30–40	$5.1 \pm 0.4$	$30 \pm 2 \pm 5$	
20–30	$8.8 \pm 0.6$	$28 \pm 2 \pm 3$	
10–20	$14.5 \pm 0.8$	$24 \pm 1 \pm 3$	
0–10	$23 \pm 1$	$22 \pm 1 \pm 2$	
$1.6 <  y  < 2.4, 3 < p_T < 6.5$ GeV/c			
50–100	$0.468 \pm 0.070$	$815 \pm 53 \pm 158$	$1397 \pm 16 \pm 166$
40–50	$2.75 \pm 0.30$	$685 \pm 50 \pm 109$	
30–40	$5.1 \pm 0.4$	$677 \pm 46 \pm 107$	
20–30	$8.8 \pm 0.6$	$572 \pm 35 \pm 85$	
10–20	$14.5 \pm 0.8$	$737 \pm 40 \pm 117$	
0–10	$23 \pm 1$	$508 \pm 29 \pm 92$	

### A.2 Nonprompt $J/\psi$

See Tables 5, 6, 7 and 8.

**Table 5** The nonprompt  $J/\psi$  fiducial cross section in bins of centrality, measured in PbPb and pp collisions at 2.76 TeV within the muon acceptance defined by Eq. (4), and the nuclear overlap function ( $T_{AA}$ , with its systematic uncertainty). Listed uncertainties are statistical first

and systematic second. A global systematic uncertainty of 3.2% (3.7%) affects all PbPb (pp) fiducial cross sections. The table corresponds to the top panel of Fig. 7

Centrality (%)	$T_{AA}$ ( $\text{mb}^{-1}$ )	PbPb $\frac{1}{T_{AA}} \frac{d^3 N_{\text{PbPb}}^{J/\psi}}{dy dp_T d\text{Cent.}}$ (pb/GeV/c)	pp $\frac{d^2 \sigma_{\text{pp}}^{J/\psi}}{dy dp_T}$ (pb/GeV/c)
$ y  < 2.4, 6.5 < p_T < 30 \text{ GeV}/c$			
50–100	$0.468 \pm 0.070$	$17 \pm 2 \pm 3$	$23.57 \pm 0.33 \pm 1.41$
40–50	$2.75 \pm 0.30$	$16 \pm 1 \pm 2$	
30–40	$5.1 \pm 0.4$	$13 \pm 1 \pm 1$	
20–30	$8.8 \pm 0.6$	$11.9 \pm 0.7 \pm 1.4$	
10–20	$14.5 \pm 0.8$	$10.4 \pm 0.5 \pm 1.3$	
0–10	$23 \pm 1$	$7.8 \pm 0.4 \pm 0.7$	

**Table 6** The nonprompt  $J/\psi$  fiducial cross section in bins of absolute rapidity, measured in PbPb and pp collisions at 2.76 TeV within the muon acceptance defined by Eq. (4), and the nuclear overlap function ( $T_{AA}$ , with its systematic uncertainty). Listed uncertainties are statis-

tical first and systematic second. A global systematic uncertainty of 6.5% (3.7%) affects all PbPb (pp) fiducial cross sections. The table corresponds to the middle panel of Fig. 7

$ y $	$T_{AA}$ ( $\text{mb}^{-1}$ )	PbPb $\frac{1}{T_{AA}} \frac{d^2 N_{\text{PbPb}}^{J/\psi}}{dy dp_T}$ (pb/GeV/c)	pp $\frac{d^2 \sigma_{\text{pp}}^{J/\psi}}{dy dp_T}$ (pb/GeV/c)
Cent. 0–100%, $6.5 < p_T < 30 \text{ GeV}/c$			
0.0–0.4	$5.67 \pm 0.32$	$10.5 \pm 0.6 \pm 1.3$	$20.0 \pm 0.7 \pm 1.3$
0.4–0.8		$12.1 \pm 0.7 \pm 1.3$	$23.8 \pm 0.8 \pm 1.9$
0.8–1.2		$11.3 \pm 0.6 \pm 0.9$	$25.2 \pm 0.8 \pm 1.4$
1.2–1.6		$13.1 \pm 0.8 \pm 1.2$	$32 \pm 1 \pm 2$
1.6–2.0		$10.7 \pm 0.8 \pm 1.0$	$29 \pm 1 \pm 2$
2.0–2.4		$4.2 \pm 0.5 \pm 0.7$	$12.2 \pm 0.7 \pm 1.2$

**Table 7** The nonprompt  $J/\psi$  fiducial cross section in bins of  $p_T$ , measured in PbPb and pp collisions at 2.76 TeV within the muon acceptance defined by Eq. (4), and the nuclear overlap function ( $T_{AA}$ , with its systematic uncertainty). Listed uncertainties are statistical first and system-

atic second. A global systematic uncertainty of 6.5% (3.7%) affects all PbPb (pp) fiducial cross sections. The table corresponds to the bottom panel of Fig. 7

$p_T$ (GeV/c)	$T_{AA}$ ( $\text{mb}^{-1}$ )	PbPb $\frac{1}{T_{AA}} \frac{d^2 N_{\text{PbPb}}^{J/\psi}}{dy dp_T}$ (pb/GeV/c)	pp $\frac{d^2 \sigma_{\text{pp}}^{J/\psi}}{dy dp_T}$ (pb/GeV/c)
Cent. 0–100%, $1.6 <  y  < 2.4$			
3–4.5	$5.67 \pm 0.32$	$46 \pm 7 \pm 8$	$61 \pm 4 \pm 14$
4.5–5.5		$43 \pm 6 \pm 6$	$63 \pm 4 \pm 6$
5.5–6.5		$31 \pm 4 \pm 4$	$57 \pm 3 \pm 5$
Cent. 0–100%, $ y  < 2.4$			
6.5–8.5	$5.67 \pm 0.32$	$52 \pm 3 \pm 4$	$111 \pm 3 \pm 9$
8.5–9.5		$39 \pm 2 \pm 3$	$80 \pm 3 \pm 5$
9.5–11		$22 \pm 1 \pm 1$	$55 \pm 2 \pm 3$
11–13		$16 \pm 1 \pm 2$	$35 \pm 1 \pm 2$
13–16		$6.0 \pm 0.5 \pm 0.8$	$16.3 \pm 0.7 \pm 0.8$
16–30		$1.071 \pm 0.082 \pm 0.203$	$3.04 \pm 0.13 \pm 0.14$



**Table 8** The nonprompt  $J/\psi$  fiducial cross section in bins of centrality, for three  $|y|$  and two  $p_T$  intervals, measured in PbPb and pp collisions at 2.76 TeV within the muon acceptance defined by Eq. (4), and the nuclear overlap function ( $T_{AA}$ , with its systematic uncertainty). Listed

uncertainties are statistical first and systematic second. A global systematic uncertainty of 3.2% (3.7%) affects all PbPb (pp) fiducial cross sections. The table corresponds to Fig. 8

Centrality (%)	$T_{AA}$ ( $\text{mb}^{-1}$ )	PbPb $\frac{1}{T_{AA}} \frac{d^3 N_{\text{PbPb}}^{J/\psi}}{dy dp_T d\text{Cent.}}$ (pb/GeV/c)	pp $\frac{d^2 \sigma_{\text{pp}}^{J/\psi}}{dy dp_T}$ (pb/GeV/c)
$0 <  y  < 1.2, 6.5 < p_T < 30 \text{ GeV}/c$			
50 $\pm$ 100	$0.468 \pm 0.070$	$18 \pm 2 \pm 4$	$23.3 \pm 0.4 \pm 1.6$
40 $\pm$ 50	$2.75 \pm 0.30$	$17 \pm 2 \pm 3$	
30 $\pm$ 40	$5.1 \pm 0.4$	$13 \pm 1 \pm 2$	
20 $\pm$ 30	$8.8 \pm 0.6$	$13 \pm 1 \pm 2$	
10 $\pm$ 20	$14.5 \pm 0.8$	$12.4 \pm 0.8 \pm 1.7$	
0 $\pm$ 10	$23 \pm 1$	$8.5 \pm 0.5 \pm 0.9$	
$1.2 <  y  < 1.6, 6.5 < p_T < 30 \text{ GeV}/c$			
50 $\pm$ 100	$0.468 \pm 0.070$	$22 \pm 4 \pm 4$	$32 \pm 1 \pm 2$
40 $\pm$ 50	$2.75 \pm 0.30$	$20 \pm 4 \pm 3$	
30 $\pm$ 40	$5.1 \pm 0.4$	$12 \pm 2 \pm 1$	
20 $\pm$ 30	$8.8 \pm 0.6$	$15 \pm 2 \pm 2$	
10 $\pm$ 20	$14.5 \pm 0.8$	$13 \pm 1 \pm 1$	
0 $\pm$ 10	$23 \pm 1$	$11 \pm 1 \pm 1$	
$1.6 <  y  < 2.4, 6.5 < p_T < 30 \text{ GeV}/c$			
50 $\pm$ 100	$0.468 \pm 0.070$	$12 \pm 2 \pm 2$	$20.3 \pm 0.6 \pm 1.5$
40 $\pm$ 50	$2.75 \pm 0.30$	$12 \pm 2 \pm 2$	
30 $\pm$ 40	$5.1 \pm 0.4$	$13 \pm 2 \pm 2$	
20 $\pm$ 30	$8.8 \pm 0.6$	$9 \pm 1 \pm 1$	
10 $\pm$ 20	$14.5 \pm 0.8$	$7.3 \pm 0.9 \pm 1.1$	
0 $\pm$ 10	$23 \pm 1$	$4.9 \pm 0.6 \pm 0.7$	
$1.6 <  y  < 2.4, 3 < p_T < 6.5 \text{ GeV}/c$			
50 $\pm$ 100	$0.468 \pm 0.070$	$163 \pm 40 \pm 37$	$179 \pm 7 \pm 23$
40 $\pm$ 50	$2.75 \pm 0.30$	$192 \pm 35 \pm 31$	
30 $\pm$ 40	$5.1 \pm 0.4$	$144 \pm 29 \pm 23$	
20 $\pm$ 30	$8.8 \pm 0.6$	$139 \pm 22 \pm 20$	
10 $\pm$ 20	$14.5 \pm 0.8$	$120 \pm 21 \pm 21$	
0 $\pm$ 10	$23 \pm 1$	$101 \pm 15 \pm 23$	

## References

1. A. Andronic et al., Heavy-flavour and quarkonium production in the LHC era: from proton–proton to heavy-ion collisions. *Eur. Phys. J. C* **76**, 107 (2016). doi:[10.1140/epjc/s10052-015-3819-5](https://doi.org/10.1140/epjc/s10052-015-3819-5). [arXiv:1506.03981](https://arxiv.org/abs/1506.03981)
2. E.V. Shuryak, Theory of hadronic plasma. *Sov. Phys. JETP* **47**, 212 (1978)
3. F. Karsch, E. Laermann, Thermodynamics and in-medium hadron properties from lattice QCD. in *Quark-Gluon Plasma III*, ed. by R.C. Hwa, X.-N. Wang (World Scientific Publishing Co. Pte. Ltd., 2004). [arXiv:hep-lat/0305025](https://arxiv.org/abs/hep-lat/0305025)
4. T. Matsui, H. Satz,  $J/\psi$  suppression by quark–gluon plasma formation. *Phys. Lett. B* **178**, 416 (1986). doi:[10.1016/0370-2693\(86\)91404-8](https://doi.org/10.1016/0370-2693(86)91404-8)
5. Y.L. Dokshitzer, D.E. Kharzeev, Heavy quark colorimetry of QCD matter. *Phys. Lett. B* **519**, 199 (2001). doi:[10.1016/S0370-2693\(01\)01130-3](https://doi.org/10.1016/S0370-2693(01)01130-3). [arXiv:hep-ph/0106202](https://arxiv.org/abs/hep-ph/0106202)
6. LHCb Collaboration, Measurement of  $J/\psi$  production in pp collisions at  $\sqrt{s} = 7$  TeV. *Eur. Phys. J. C* **71**, 1645 (2011). doi:[10.1140/epjc/s10052-011-1645-y](https://doi.org/10.1140/epjc/s10052-011-1645-y). [arXiv:1103.0423](https://arxiv.org/abs/1103.0423)
7. CMS Collaboration, Prompt and non-prompt  $J/\psi$  production in pp collisions at  $\sqrt{s} = 7$  TeV. *Eur. Phys. J. C* **71**, 1575 (2011). doi:[10.1140/epjc/s10052-011-1575-8](https://doi.org/10.1140/epjc/s10052-011-1575-8). [arXiv:1011.4193](https://arxiv.org/abs/1011.4193)
8. ATLAS Collaboration, Measurement of the differential cross-sections of inclusive, prompt and non-prompt  $J/\psi$  production in pp collisions at  $\sqrt{s} = 7$  TeV. *Nucl. Phys. B* **850**, 387 (2011). doi:[10.1016/j.nuclphysb.2011.05.015](https://doi.org/10.1016/j.nuclphysb.2011.05.015). [arXiv:1104.3038](https://arxiv.org/abs/1104.3038)
9. Á. Mócsy, P. Petreczky, Color screening melts quarkonium. *Phys. Rev. Lett.* **99**, 211602 (2007). doi:[10.1103/PhysRevLett.99.211602](https://doi.org/10.1103/PhysRevLett.99.211602). [arXiv:0706.2183](https://arxiv.org/abs/0706.2183)
10. E. Braaten, M.H. Thoma, Energy loss of a heavy quark in the quark–gluon plasma. *Phys. Rev. D* **44**, R2625 (1991). doi:[10.1103/PhysRevD.44.R2625](https://doi.org/10.1103/PhysRevD.44.R2625)

11. B.-W. Zhang, E. Wang, X.-N. Wang, Heavy quark energy loss in nuclear medium. *Phys. Rev. Lett.* **93**, 072301 (2004). doi:[10.1103/PhysRevLett.93.072301](https://doi.org/10.1103/PhysRevLett.93.072301). arXiv:[nucl-th/0309040](https://arxiv.org/abs/nucl-th/0309040)
12. N. Armesto, A. Dainese, C.A. Salgado, U.A. Wiedemann, Testing the color charge and mass dependence of parton energy loss with heavy-to-light ratios at BNL RHIC and CERN LHC. *Phys. Rev. D* **71**, 054027 (2005). doi:[10.1103/PhysRevD.71.054027](https://doi.org/10.1103/PhysRevD.71.054027). arXiv:[hep-ph/0501225](https://arxiv.org/abs/hep-ph/0501225)
13. H. van Hees, V. Greco, R. Rapp, Heavy-quark probes of the quark–gluon plasma at RHIC. *Phys. Rev. C* **73**, 034913 (2006). doi:[10.1103/PhysRevC.73.034913](https://doi.org/10.1103/PhysRevC.73.034913). arXiv:[nucl-th/0508055](https://arxiv.org/abs/nucl-th/0508055)
14. S. Peigne, A. Peshier, Collisional energy loss of a fast heavy quark in a quark–gluon plasma. *Phys. Rev. D* **77**, 114017 (2008). doi:[10.1103/PhysRevD.77.114017](https://doi.org/10.1103/PhysRevD.77.114017). arXiv:[0802.4364](https://arxiv.org/abs/0802.4364)
15. S. Wicks, W. Horowitz, M. Djordjevic, M. Gyulassy, Heavy quark jet quenching with collisional plus radiative energy loss and path length fluctuations. *Nucl. Phys. A* **783**, 493 (2007). doi:[10.1016/j.nuclphysa.2006.11.102](https://doi.org/10.1016/j.nuclphysa.2006.11.102). arXiv:[nucl-th/0701063](https://arxiv.org/abs/nucl-th/0701063)
16. P.B. Gossiaux, J. Aichelin, T. Gousset, V. Guiho, Competition of heavy-quark radiative and collisional energy loss in deconfined matter. *J. Phys. G* **37**, 094019 (2010). doi:[10.1088/0954-3899/37/9/094019](https://doi.org/10.1088/0954-3899/37/9/094019). arXiv:[1001.4166](https://arxiv.org/abs/1001.4166)
17. A. Adil, I. Vitev, Collisional dissociation of heavy mesons in dense QCD matter. *Phys. Lett. B* **649**, 139 (2007). doi:[10.1016/j.physletb.2007.03.050](https://doi.org/10.1016/j.physletb.2007.03.050). arXiv:[hep-ph/0611109](https://arxiv.org/abs/hep-ph/0611109)
18. R. Sharma, I. Vitev, B.-W. Zhang, Light-cone wave function approach to open heavy flavor dynamics in QCD matter. *Phys. Rev. C* **80**, 054902 (2009). doi:[10.1103/PhysRevC.80.054902](https://doi.org/10.1103/PhysRevC.80.054902). arXiv:[0904.0032](https://arxiv.org/abs/0904.0032)
19. H. Satz, Calibrating the in-medium behavior of quarkonia. *Adv. High Energy Phys.* **2013**, 242918 (2013). doi:[10.1155/2013/242918](https://doi.org/10.1155/2013/242918). arXiv:[1303.3493](https://arxiv.org/abs/1303.3493)
20. F. Riek, R. Rapp, Quarkonia and heavy-quark relaxation times in the quark–gluon plasma. *Phys. Rev. C* **82**, 035201 (2010). doi:[10.1103/PhysRevC.82.035201](https://doi.org/10.1103/PhysRevC.82.035201). arXiv:[1005.0769](https://arxiv.org/abs/1005.0769)
21. R. Sharma, I. Vitev, High transverse momentum quarkonium production and dissociation in heavy ion collisions. *Phys. Rev. C* **87**, 044905 (2013). doi:[10.1103/PhysRevC.87.044905](https://doi.org/10.1103/PhysRevC.87.044905). arXiv:[1203.0329](https://arxiv.org/abs/1203.0329)
22. CMS Collaboration, Suppression of non-prompt  $J/\psi$ , prompt  $J/\psi$ , and  $\Upsilon(1S)$  in PbPb collisions at  $\sqrt{s_{NN}} = 2.76$  TeV. *JHEP* **05**, 063 (2012). doi:[10.1007/JHEP05\(2012\)063](https://doi.org/10.1007/JHEP05(2012)063). arXiv:[1201.5069](https://arxiv.org/abs/1201.5069)
23. ALICE Collaboration, Inclusive, prompt and non-prompt  $J/\psi$  production at mid-rapidity in Pb–Pb collisions at  $\sqrt{s_{NN}} = 2.76$  TeV. *JHEP* **07**, 051 (2015). doi:[10.1007/JHEP07\(2015\)051](https://doi.org/10.1007/JHEP07(2015)051). arXiv:[1504.07151](https://arxiv.org/abs/1504.07151)
24. ALICE Collaboration,  $J/\psi$  suppression at forward rapidity in Pb–Pb collisions at  $\sqrt{s_{NN}} = 2.76$  TeV. *Phys. Rev. Lett.* **109**, 072301 (2012). doi:[10.1103/PhysRevLett.109.072301](https://doi.org/10.1103/PhysRevLett.109.072301). arXiv:[1202.1383](https://arxiv.org/abs/1202.1383)
25. PHENIX Collaboration,  $J/\psi$  suppression at forward rapidity in AuAu collisions at  $\sqrt{s_{NN}} = 200$  GeV. *Phys. Rev. C* **84**, 054912 (2011). doi:[10.1103/PhysRevC.84.054912](https://doi.org/10.1103/PhysRevC.84.054912). arXiv:[1103.6269](https://arxiv.org/abs/1103.6269)
26. ALICE Collaboration, Differential studies of inclusive  $J/\psi$  and  $\psi(2S)$  production at forward rapidity in Pb–Pb collisions at  $\sqrt{s_{NN}} = 2.76$  TeV. *JHEP* **05**, 179 (2016). doi:[10.1007/JHEP05\(2016\)179](https://doi.org/10.1007/JHEP05(2016)179). arXiv:[1506.08804](https://arxiv.org/abs/1506.08804)
27. X. Zhao, R. Rapp, Medium modifications and production of charmonia at LHC. *Nucl. Phys. A* **859**, 114 (2011). doi:[10.1016/j.nuclphysa.2011.05.001](https://doi.org/10.1016/j.nuclphysa.2011.05.001). arXiv:[1102.2194](https://arxiv.org/abs/1102.2194)
28. A. Andronic, P. Braun-Munzinger, K. Redlich, J. Stachel, The thermal model on the verge of the ultimate test: particle production in Pb–Pb collisions at the LHC. *J. Phys. G* **38**, 124081 (2011). doi:[10.1088/0954-3899/38/12/124081](https://doi.org/10.1088/0954-3899/38/12/124081). arXiv:[1106.6321](https://arxiv.org/abs/1106.6321)
29. E.G. Ferreira, Charmonium dissociation and recombination at LHC: revisiting comovers. *Phys. Lett. B* **731**, 57 (2014). doi:[10.1016/j.physletb.2014.02.011](https://doi.org/10.1016/j.physletb.2014.02.011). arXiv:[1210.3209](https://arxiv.org/abs/1210.3209)
30. J.-Y. Ollitrault, Anisotropy as a signature of transverse collective flow. *Phys. Rev. D* **46**, 229 (1992). doi:[10.1103/PhysRevD.46.229](https://doi.org/10.1103/PhysRevD.46.229)
31. ALICE Collaboration, Azimuthal anisotropy of D meson production in Pb–Pb collisions at  $\sqrt{s_{NN}} = 2.76$  TeV. *Phys. Rev. C* **90**, 034904 (2014). doi:[10.1103/PhysRevC.90.034904](https://doi.org/10.1103/PhysRevC.90.034904). arXiv:[1405.2001](https://arxiv.org/abs/1405.2001)
32. ALICE Collaboration,  $J/\psi$  elliptic flow in PbPb collisions at  $\sqrt{s_{NN}} = 2.76$  TeV. *Phys. Rev. Lett.* **111**, 162301 (2013). doi:[10.1103/PhysRevLett.111.162301](https://doi.org/10.1103/PhysRevLett.111.162301). arXiv:[1303.5880](https://arxiv.org/abs/1303.5880)
33. P. Braun-Munzinger, J. Stachel, (Non)thermal aspects of charmonium production and a new look at  $J/\psi$  suppression. *Phys. Lett. B* **490**, 196 (2000). doi:[10.1016/S0370-2693\(00\)00991-6](https://doi.org/10.1016/S0370-2693(00)00991-6). arXiv:[nucl-th/0007059](https://arxiv.org/abs/nucl-th/0007059)
34. Y. Liu, Z. Qu, N. Xu, P. Zhuang,  $J/\psi$  transverse momentum distribution in high energy nuclear collisions at RHIC. *Phys. Lett. B* **678**, 72 (2009). doi:[10.1016/j.physletb.2009.06.006](https://doi.org/10.1016/j.physletb.2009.06.006). arXiv:[0901.2757](https://arxiv.org/abs/0901.2757)
35. CMS Collaboration, The CMS experiment at the CERN LHC. *JINST* **3**, S08004 (2008). doi:[10.1088/1748-0221/3/08/S08004](https://doi.org/10.1088/1748-0221/3/08/S08004)
36. CMS Collaboration, Observation and studies of jet quenching in PbPb collisions at  $\sqrt{s_{NN}} = 2.76$  TeV. *Phys. Rev. C* **84**, 024906 (2011). doi:[10.1103/PhysRevC.84.024906](https://doi.org/10.1103/PhysRevC.84.024906). arXiv:[1102.1957](https://arxiv.org/abs/1102.1957)
37. CMS Collaboration, Luminosity calibration for the 2013 proton–lead and proton–proton data taking. CMS Physics Analysis Summary CMS-PAS-LUM-13-002, 2013
38. C. Roland, Track reconstruction in heavy ion collisions with the CMS silicon tracker. in *TIME 20005—Proceedings of the 1st Workshop on Tracking in High Multiplicity Environments*. 2006. doi:[10.1016/j.nima.2006.05.023](https://doi.org/10.1016/j.nima.2006.05.023). [*Nucl. Instrum. Meth. A* **566** (2006) **123**]
39. CMS Collaboration, Description and performance of track and primary-vertex reconstruction with the CMS tracker. *JINST* **9**, P10009 (2014). doi:[10.1088/1748-0221/9/10/P10009](https://doi.org/10.1088/1748-0221/9/10/P10009). arXiv:[1405.6569](https://arxiv.org/abs/1405.6569)
40. M.L. Miller, K. Reygers, S.J. Sanders, P. Steinberg, Glauber modeling in high-energy nuclear collisions. *Ann. Rev. Nucl. Part. Sci.* **57**, 205 (2007). doi:[10.1146/annurev.nucl.57.090506.123020](https://doi.org/10.1146/annurev.nucl.57.090506.123020). arXiv:[nucl-ex/0701025](https://arxiv.org/abs/nucl-ex/0701025)
41. T. Sjöstrand, S. Mrenna, P.Z. Skands, PYTHIA 6.4 physics and manual. *JHEP* **05**, 026 (2006). doi:[10.1088/1126-6708/2006/05/026](https://doi.org/10.1088/1126-6708/2006/05/026). arXiv:[hep-ph/0603175](https://arxiv.org/abs/hep-ph/0603175)
42. D.J. Lange, The EvtGen particle decay simulation package. *Nucl. Instrum. Methods A* **462**, 152 (2001). doi:[10.1016/S0168-9002\(01\)00089-4](https://doi.org/10.1016/S0168-9002(01)00089-4)
43. E. Barberio, Z. Was, PHOTOS—a universal Monte Carlo for QED radiative corrections: version 2.0. *Comput. Phys. Commun.* **79**, 291 (1994). doi:[10.1016/0010-4655\(94\)90074-4](https://doi.org/10.1016/0010-4655(94)90074-4)
44. ALICE Collaboration,  $J/\psi$  polarization in pp collisions at  $\sqrt{s} = 7$  TeV. *Phys. Rev. Lett.* **108**, 082001 (2012). doi:[10.1103/PhysRevLett.108.082001](https://doi.org/10.1103/PhysRevLett.108.082001). arXiv:[1111.1630](https://arxiv.org/abs/1111.1630)
45. CMS Collaboration, Measurement of the prompt  $J/\psi$  and  $\psi(2S)$  polarizations in pp collisions at  $\sqrt{s} = 7$  TeV. *Phys. Lett. B* **727**, 381 (2013). doi:[10.1016/j.physletb.2013.10.055](https://doi.org/10.1016/j.physletb.2013.10.055). arXiv:[1307.6070](https://arxiv.org/abs/1307.6070)
46. LHCb Collaboration, Measurement of  $J/\psi$  polarization in pp collisions at  $\sqrt{s} = 7$  TeV. *Eur. Phys. J. C* **73**, 2631 (2013). doi:[10.1140/epjc/s10052-013-2631-3](https://doi.org/10.1140/epjc/s10052-013-2631-3). arXiv:[1307.6379](https://arxiv.org/abs/1307.6379)
47. CMS Collaboration, Indications of suppression of excited  $\Upsilon$  states in PbPb collisions at  $\sqrt{s_{NN}} = 2.76$  TeV. *Phys. Rev. Lett.* **107**, 052302 (2011). doi:[10.1103/PhysRevLett.107.052302](https://doi.org/10.1103/PhysRevLett.107.052302). arXiv:[1105.4894](https://arxiv.org/abs/1105.4894)
48. CMS Collaboration, Observation of sequential Upsilon suppression in PbPb collisions. *Phys. Rev. Lett.* **109**, 222301 (2012). doi:[10.1103/PhysRevLett.109.222301](https://doi.org/10.1103/PhysRevLett.109.222301). arXiv:[1208.2826](https://arxiv.org/abs/1208.2826)
49. CMS Collaboration, Event activity dependence of  $\Upsilon(nS)$  production in  $\sqrt{s_{NN}} = 5.02$  TeV pPb and  $\sqrt{s} = 2.76$  TeV pp collisions. *JHEP* **04**, 103 (2014). doi:[10.1007/JHEP04\(2014\)103](https://doi.org/10.1007/JHEP04(2014)103). arXiv:[1312.6300](https://arxiv.org/abs/1312.6300)

50. CMS Collaboration, Measurement of prompt  $\psi(2S) \rightarrow J/\psi$  yield ratios in PbPb and  $pp$  collisions at  $\sqrt{s_{NN}} = 2.76$  TeV. *Phys. Rev. Lett.* **113**, 262301 (2014). doi:[10.1103/PhysRevLett.113.262301](https://doi.org/10.1103/PhysRevLett.113.262301). arXiv:[1410.1804](https://arxiv.org/abs/1410.1804)
51. I.P. Lokhtin, A.M. Snigirev, A model of jet quenching in ultrarelativistic heavy ion collisions and high- $p_T$  hadron spectra at RHIC. *Eur. Phys. J. C* **45**, 211 (2006). doi:[10.1140/epjc/s2005-02426-3](https://doi.org/10.1140/epjc/s2005-02426-3). arXiv:[hep-ph/0506189](https://arxiv.org/abs/hep-ph/0506189)
52. GEANT4 Collaboration, GEANT4—a simulation toolkit. *Nucl. Instrum. Methods A* **506**, 250 (2003). doi:[10.1016/S0168-9002\(03\)01368-8](https://doi.org/10.1016/S0168-9002(03)01368-8)
53. CMS Collaboration, Performance of CMS muon reconstruction in  $pp$  collision events at  $\sqrt{s} = 7$  TeV. *JINST* **7**, P10002 (2012). doi:[10.1088/1748-0221/7/10/P10002](https://doi.org/10.1088/1748-0221/7/10/P10002). arXiv:[1206.4071](https://arxiv.org/abs/1206.4071)
54. CMS Collaboration, Dependence on pseudorapidity and centrality of charged hadron production in PbPb collisions at  $\sqrt{s_{NN}} = 2.76$  TeV. *JHEP* **08**, 141 (2011). doi:[10.1007/JHEP08\(2011\)141](https://doi.org/10.1007/JHEP08(2011)141). arXiv:[1107.4800](https://arxiv.org/abs/1107.4800)
55. ALEPH Collaboration, Measurement of the anti- $B^0$  and  $B^-$  meson lifetimes. *Phys. Lett. B* **307**, 194 (1993). doi:[10.1016/0370-2693\(93\)90211-Y](https://doi.org/10.1016/0370-2693(93)90211-Y). [Erratum: *Phys. Lett. B* **325**, 537 (1994)]
56. CMS Collaboration,  $J/\psi$  and  $\psi(2S)$  production in  $pp$  collisions at  $\sqrt{s} = 7$  TeV. *JHEP* **02**, 011 (2012). doi:[10.1007/JHEP02\(2012\)011](https://doi.org/10.1007/JHEP02(2012)011). arXiv:[1111.1557](https://arxiv.org/abs/1111.1557)
57. M. Oreglia, A study of the reactions  $\psi' \rightarrow \gamma\gamma\psi$ . PhD thesis, SLAC (1980)
58. ALICE Collaboration, Measurement of the elliptic anisotropy of charged particles produced in PbPb collisions at nucleon–nucleon center-of-mass energy = 2.76 TeV. *Phys. Rev. C* **87**, 014902 (2013). doi:[10.1103/PhysRevC.87.014902](https://doi.org/10.1103/PhysRevC.87.014902). arXiv:[1204.1409](https://arxiv.org/abs/1204.1409)
59. A.M. Poskanzer, S.A. Voloshin, Methods for analyzing anisotropic flow in relativistic nuclear collisions. *Phys. Rev. C* **58**, 1671 (1998). doi:[10.1103/PhysRevC.58.1671](https://doi.org/10.1103/PhysRevC.58.1671). arXiv:[nucl-ex/9805001](https://arxiv.org/abs/nucl-ex/9805001)
60. CMS Collaboration, Azimuthal anisotropy of charged particles at high transverse momenta in PbPb collisions at  $\sqrt{s_{NN}} = 2.76$  TeV. *Phys. Rev. Lett.* **109**, 022301 (2012). doi:[10.1103/PhysRevLett.109.022301](https://doi.org/10.1103/PhysRevLett.109.022301). arXiv:[1204.1850](https://arxiv.org/abs/1204.1850)
61. ALICE Collaboration, Suppression of high transverse momentum D mesons in central Pb–Pb collisions at  $\sqrt{s_{NN}} = 2.76$  TeV. *JHEP* **09**, 112 (2012). doi:[10.1007/JHEP09\(2012\)112](https://doi.org/10.1007/JHEP09(2012)112). arXiv:[1203.2160](https://arxiv.org/abs/1203.2160)
62. ALICE Collaboration, Centrality dependence of high- $p_T$  D meson suppression in Pb–Pb collisions at  $\sqrt{s_{NN}} = 2.76$  TeV. *JHEP* **11**, 205 (2015). doi:[10.1007/JHEP11\(2015\)205](https://doi.org/10.1007/JHEP11(2015)205). arXiv:[1506.06604](https://arxiv.org/abs/1506.06604)
63. F. Arleo, R. Kolevatov, S. Peigné, M. Rustamova, Centrality and  $p_\perp$  dependence of  $J/\psi$  suppression in proton–nucleus collisions from parton energy loss. *JHEP* **05**, 155 (2013). doi:[10.1007/JHEP05\(2013\)155](https://doi.org/10.1007/JHEP05(2013)155). arXiv:[1304.0901](https://arxiv.org/abs/1304.0901)
64. E.G. Ferreira, Excited charmonium suppression in proton–nucleus collisions as a consequence of comovers. *Phys. Lett. B* **749**, 98 (2015). doi:[10.1016/j.physletb.2015.07.066](https://doi.org/10.1016/j.physletb.2015.07.066). arXiv:[1411.0549](https://arxiv.org/abs/1411.0549)
65. H. Fujii, K. Watanabe, Heavy quark pair production in high energy pA collisions: quarkonium. *Nucl. Phys. A* **915**, 1 (2013). doi:[10.1016/j.nuclphysa.2013.06.011](https://doi.org/10.1016/j.nuclphysa.2013.06.011). arXiv:[1304.2221](https://arxiv.org/abs/1304.2221)
66. ALICE Collaboration, Centrality dependence of inclusive  $J/\psi$  production in p–Pb collisions at  $\sqrt{s_{NN}} = 5.02$  TeV. *JHEP* **11**, 127 (2015). doi:[10.1007/JHEP11\(2015\)127](https://doi.org/10.1007/JHEP11(2015)127). arXiv:[1506.08808](https://arxiv.org/abs/1506.08808)
67. ALICE Collaboration, Rapidity and transverse-momentum dependence of the inclusive  $J/\psi$  nuclear modification factor in p–Pb collisions at  $\sqrt{s_{NN}} = 5.02$  TeV. *JHEP* **06**, 055 (2015). doi:[10.1007/JHEP06\(2015\)055](https://doi.org/10.1007/JHEP06(2015)055). arXiv:[1503.07](https://arxiv.org/abs/1503.07)
68. P. Faccioli, C. Lourenco, J. Seixas, H.K. Woehri, Study of  $\psi(2S)$  and  $\chi_c$  decays as feed-down sources of  $J/\psi$  hadroproduction. *JHEP* **10**, 004 (2008). doi:[10.1088/1126-6708/2008/10/004](https://doi.org/10.1088/1126-6708/2008/10/004). arXiv:[0809.2153](https://arxiv.org/abs/0809.2153)
69. LHCb Collaboration, Measurement of the ratio of prompt  $\chi_c$  to  $J/\psi$  production in  $pp$  collisions at  $\sqrt{s} = 7$  TeV. *Phys. Lett. B* **718**, 431 (2012). doi:[10.1016/j.physletb.2012.10.068](https://doi.org/10.1016/j.physletb.2012.10.068). arXiv:[1204.1462](https://arxiv.org/abs/1204.1462)
70. M. He, R.J. Fries, R. Rapp, Heavy flavor at the Large Hadron Collider in a strong coupling approach. *Phys. Lett. B* **735**, 445 (2014). doi:[10.1016/j.physletb.2014.05.050](https://doi.org/10.1016/j.physletb.2014.05.050). arXiv:[1401.3817](https://arxiv.org/abs/1401.3817)
71. ALICE Collaboration, Transverse momentum dependence of D-meson production in Pb–Pb collisions at  $\sqrt{s_{NN}} = 2.76$  TeV. *JHEP* **03**, 081 (2016). doi:[10.1007/JHEP03\(2016\)081](https://doi.org/10.1007/JHEP03(2016)081). arXiv:[1509.06888](https://arxiv.org/abs/1509.06888)
72. Y.L. Dokshitzer, V.A. Khoze, S.I. Troian, On specific QCD properties of heavy quark fragmentation ('dead cone'). *J. Phys. G* **17**, 1602 (1991). doi:[10.1088/0954-3899/17/10/023](https://doi.org/10.1088/0954-3899/17/10/023)
73. N. Armesto, C.A. Salgado, U.A. Wiedemann, Medium induced gluon radiation off massive quarks fills the dead cone. *Phys. Rev. D* **69**, 114003 (2004). doi:[10.1103/PhysRevD.69.114003](https://doi.org/10.1103/PhysRevD.69.114003). arXiv:[hep-ph/0312106](https://arxiv.org/abs/hep-ph/0312106)
74. M. Djordjevic, M. Gyulassy, Heavy quark radiative energy loss in QCD matter. *Nucl. Phys. A* **733**, 265 (2004). doi:[10.1016/j.nuclphysa.2003.12.020](https://doi.org/10.1016/j.nuclphysa.2003.12.020). arXiv:[nucl-th/0310076](https://arxiv.org/abs/nucl-th/0310076)
75. CMS Collaboration, Evidence of  $b$ -jet quenching in PbPb collisions at  $\sqrt{s_{NN}} = 2.76$  TeV. *Phys. Rev. Lett.* **113**, 132301 (2014). doi:[10.1103/PhysRevLett.113.132301](https://doi.org/10.1103/PhysRevLett.113.132301). arXiv:[1312.4198](https://arxiv.org/abs/1312.4198). [Erratum: *Phys. Rev. Lett.* **115**, 029903 (2015)]
76. M. Djordjevic, Heavy flavor puzzle at LHC: a serendipitous interplay of jet suppression and fragmentation. *Phys. Rev. Lett.* **112**, 042302 (2014). doi:[10.1103/PhysRevLett.112.042302](https://doi.org/10.1103/PhysRevLett.112.042302). arXiv:[1307.4702](https://arxiv.org/abs/1307.4702)

**CMS Collaboration****Yerevan Physics Institute, Yerevan, Armenia**

V. Khachatryan, A. M. Sirunyan, A. Tumasyan

**Institut für Hochenergiephysik, Wien, Austria**W. Adam, E. Asilar, T. Bergauer, J. Brandstetter, E. Brondolin, M. Dragicevic, J. Erö, M. Flechl, M. Friedl, R. Frühwirth<sup>1</sup>, V. M. Ghete, C. Hartl, N. Hörmann, J. Hrubec, M. Jeitler<sup>1</sup>, A. König, I. Krätschmer, D. Liko, T. Matsushita, I. Mikulec, D. Rabady, N. Rad, B. Rahbaran, H. Rohringer, J. Schieck<sup>1</sup>, J. Strauss, W. Waltenberger, C.-E. Wulz<sup>1</sup>**Institute for Nuclear Problems, Minsk, Belarus**

O. Dvornikov, V. Makarenko, V. Zykunov

**National Centre for Particle and High Energy Physics, Minsk, Belarus**

V. Mossolov, N. Shumeiko, J. Suarez Gonzalez

**Universiteit Antwerpen, Antwerpen, Belgium**

S. Alderweireldt, E. A. De Wolf, X. Janssen, J. Lauwers, M. Van De Klundert, H. Van Haevermaet, P. Van Mechelen, N. Van Remortel, A. Van Spilbeeck

**Vrije Universiteit Brussel, Brussel, Belgium**

S. Abu Zeid, F. Blekman, J. D'Hondt, N. Daci, I. De Bruyn, K. Deroover, S. Lowette, S. Moortgat, L. Moreels, A. Olbrechts, Q. Python, S. Tavernier, W. Van Doninck, P. Van Mulders, I. Van Parijs

**Université Libre de Bruxelles, Bruxelles, Belgium**H. Brun, B. Clerbaux, G. De Lentdecker, H. Delannoy, G. Fasanella, L. Favart, R. Goldouzian, A. Grebenyuk, G. Karapostoli, T. Lenzi, A. Léonard, J. Luetic, T. Maerschalk, A. Marinov, A. Randle-conde, T. Seva, C. Vander Velde, P. Vanlaer, D. Vannerom, R. Yonamine, F. Zenoni, F. Zhang<sup>2</sup>**Ghent University, Ghent, Belgium**

A. Cimmino, T. Cornelis, D. Dobur, A. Fagot, G. Garcia, M. Gul, I. Khvastunov, D. Poyraz, S. Salva, R. Schöfbeck, A. Sharma, M. Tytgat, W. Van Driessche, E. Yazgan, N. Zaganidis

**Université Catholique de Louvain, Louvain-la-Neuve, Belgium**H. Bakhshiansohi, C. Beluffi<sup>3</sup>, O. Bondu, S. Brochet, G. Bruno, A. Caudron, S. De Visscher, C. Delaere, M. Delcourt, B. Francois, A. Giammanco, A. Jafari, P. Jez, M. Komm, G. Krintiras, V. Lemaître, A. Magitteri, A. Mertens, M. Musich, C. Nuttens, K. Piotrkowski, L. Quertenmont, M. Selvaggi, M. Vidal Marono, S. Wertz**Université de Mons, Mons, Belgium**

N. Bely

**Centro Brasileiro de Pesquisas Fisicas, Rio de Janeiro, Brazil**

W. L. Aldá Júnior, F. L. Alves, G. A. Alves, L. Brito, C. Hensel, A. Moraes, M. E. Pol, P. Rebello Teles

**Universidade do Estado do Rio de Janeiro, Rio de Janeiro, Brazil**E. Belchior Batista Das Chagas, W. Carvalho, J. Chinellato<sup>4</sup>, A. Custódio, E. M. Da Costa, G. G. Da Silveira<sup>5</sup>, D. De Jesus Damiao, C. De Oliveira Martins, S. Fonseca De Souza, L. M. Huertas Guativa, H. Malbouisson, D. Matos Figueiredo, C. Mora Herrera, L. Mundim, H. Nogima, W. L. Prado Da Silva, A. Santoro, A. Sznajder, E. J. Tonelli Manganote<sup>4</sup>, A. Vilela Pereira**Universidade Estadual Paulista<sup>a</sup>, Universidade Federal do ABC<sup>b</sup>, São Paulo, Brazil**S. Ahuja<sup>a</sup>, C. A. Bernardes<sup>b</sup>, S. Dogra<sup>a</sup>, T. R. Fernandez Perez Tomei<sup>a</sup>, E. M. Gregores<sup>b</sup>, P. G. Mercadante<sup>b</sup>, C. S. Moon<sup>a</sup>, S. F. Novaes<sup>a</sup>, Sandra S. Padula<sup>a</sup>, D. Romero Abad<sup>b</sup>, J. C. Ruiz Vargas**Institute for Nuclear Research and Nuclear Energy, Sofia, Bulgaria**

A. Aleksandrov, R. Hadjiiska, P. Iaydjiev, M. Rodozov, S. Stoykova, G. Sultanov, M. Vutova

**University of Sofia, Sofia, Bulgaria**

A. Dimitrov, I. Glushkov, L. Litov, B. Pavlov, P. Petkov



**Beihang University, Beijing, China**W. Fang<sup>6</sup>**Institute of High Energy Physics, Beijing, China**M. Ahmad, J. G. Bian, G. M. Chen, H. S. Chen, M. Chen, Y. Chen<sup>7</sup>, T. Cheng, C. H. Jiang, D. Leggat, Z. Liu, F. Romeo, S. M. Shaheen, A. Spiezia, J. Tao, C. Wang, Z. Wang, H. Zhang, J. Zhao**State Key Laboratory of Nuclear Physics and Technology, Peking University, Beijing, China**

Y. Ban, G. Chen, Q. Li, S. Liu, Y. Mao, S. J. Qian, D. Wang, Z. Xu

**Universidad de Los Andes, Bogota, Colombia**

C. Avila, A. Cabrera, L. F. Chaparro Sierra, C. Florez, J. P. Gomez, C. F. González Hernández, J. D. Ruiz Alvarez, J. C. Sanabria

**University of Split, Faculty of Electrical Engineering, Mechanical Engineering and Naval Architecture, Split, Croatia**

N. Godinovic, D. Lelas, I. Puljak, P. M. Ribeiro Cipriano, T. Sculac

**University of Split, Faculty of Science, Split, Croatia**

Z. Antunovic, M. Kovac

**Institute Rudjer Boskovic, Zagreb, Croatia**

V. Brigljevic, D. Ferencek, K. Kadija, S. Micanovic, L. Sudic, T. Susa

**University of Cyprus, Nicosia, Cyprus**

A. Attikis, G. Mavromanolakis, J. Mousa, C. Nicolaou, F. Ptochos, P. A. Razis, H. Rykaczewski, D. Tsiakkouri

**Charles University, Prague, Czech Republic**M. Finger<sup>8</sup>, M. Finger Jr.<sup>8</sup>**Universidad San Francisco de Quito, Quito, Ecuador**

E. Carrera Jarrin

**Academy of Scientific Research and Technology of the Arab Republic of Egypt, Egyptian Network of High Energy Physics, Cairo, Egypt**A. Ellithi Kamel<sup>9</sup>, M. A. Mahmoud<sup>10,11</sup>, A. Radi<sup>11,12</sup>**National Institute of Chemical Physics and Biophysics, Tallinn, Estonia**

M. Kadastik, L. Perrini, M. Raidal, A. Tiko, C. Veelken

**Department of Physics, University of Helsinki, Helsinki, Finland**

P. Eerola, J. Pekkanen, M. Voutilainen

**Helsinki Institute of Physics, Helsinki, Finland**

J. Härkönen, T. Järvinen, V. Karimäki, R. Kinnunen, T. Lampén, K. Lassila-Perini, S. Lehti, T. Lindén, P. Luukka, J. Tuominiemi, E. Tuovinen, L. Wendland

**Lappeenranta University of Technology, Lappeenranta, Finland**

J. Talvitie, T. Tuuva

**IRFU, CEA, Université Paris-Saclay, Gif-sur-Yvette, France**

M. Besancon, F. Couderc, M. Dejardin, D. Denegri, B. Fabbro, J. L. Faure, C. Favaro, F. Ferri, S. Ganjour, S. Ghosh, A. Givernaud, P. Gras, G. Hamel de Monchenault, P. Jarry, I. Kucher, E. Locci, M. Machet, J. Malcles, J. Rander, A. Rosowsky, M. Titov, A. Zghiche

**Laboratoire Leprince-Ringuet, Ecole Polytechnique, IN2P3-CNRS, Palaiseau, France**

A. Abdulsalam, I. Antropov, S. Baffioni, F. Beaudette, P. Busson, L. Cadamuro, E. Chapon, C. Charlot, O. Davignon, R. Granier de Cassagnac, M. Jo, S. Lisniak, P. Miné, M. Nguyen, C. Ochando, G. Ortona, P. Paganini, P. Pigard, S. Regnard, R. Salerno, Y. Sirois, T. Strebler, Y. Yilmaz, A. Zabi

**Institut Pluridisciplinaire Hubert Curien, Université de Strasbourg, Université de Haute Alsace Mulhouse, CNRS/IN2P3, Strasbourg, France**

J.-L. Agram<sup>13</sup>, J. Andrea, A. Aubin, D. Bloch, J.-M. Brom, M. Buttignol, E. C. Chabert, N. Chanon, C. Collard, E. Conte<sup>13</sup>, X. Coubez, J.-C. Fontaine<sup>13</sup>, D. Gelé, U. Goerlach, A.-C. Le Bihan, K. Skovpen, P. Van Hove

**Centre de Calcul de l'Institut National de Physique Nucleaire et de Physique des Particules, CNRS/IN2P3, Villeurbanne, France**

S. Gadrat

**Université de Lyon, Université Claude Bernard Lyon 1, CNRS-IN2P3, Institut de Physique Nucléaire de Lyon, Villeurbanne, France**

S. Beauceron, C. Bernet, G. Boudoul, E. Bouvier, C. A. Carrillo Montoya, R. Chierici, D. Contardo, B. Courbon, P. Depasse, H. El Mamouni, J. Fan, J. Fay, S. Gascon, M. Gouzevitch, G. Grenier, B. Ille, F. Lagarde, I. B. Laktineh, M. Lethuillier, L. Mirabito, A. L. Pequegnot, S. Perries, A. Popov<sup>14</sup>, D. Sabes, V. Sordini, M. Vander Donckt, P. Verdier, S. Viret

**Georgian Technical University, Tbilisi, Georgia**

T. Toriashvili<sup>15</sup>

**Tbilisi State University, Tbilisi, Georgia**

D. Lomidze

**RWTH Aachen University, I. Physikalisches Institut, Aachen, Germany**

C. Autermann, S. Beranek, L. Feld, A. Heister, M. K. Kiesel, K. Klein, M. Lipinski, A. Ostapchuk, M. Preuten, F. Raupach, S. Schael, C. Schomakers, J. Schulz, T. Verlage, H. Weber, V. Zhukov<sup>14</sup>

**RWTH Aachen University, III. Physikalisches Institut A, Aachen, Germany**

A. Albert, M. Brodski, E. Dietz-Laursonn, D. Duchardt, M. Endres, M. Erdmann, S. Erdweg, T. Esch, R. Fischer, A. Güth, M. Hamer, T. Hebbeker, C. Heidemann, K. Hoepfner, S. Knutzen, M. Merschmeyer, A. Meyer, P. Millet, S. Mukherjee, M. Olschewski, K. Padeken, T. Pook, M. Radziej, H. Reithler, M. Rieger, F. Scheuch, L. Sonnenschein, D. Teysier, S. Thüer

**RWTH Aachen University, III. Physikalisches Institut B, Aachen, Germany**

V. Cherepanov, G. Flügge, B. Kargoll, T. Kress, A. Künsken, J. Lingemann, T. Müller, A. Nehr Korn, A. Nowack, C. Pistone, O. Pooth, A. Stahl<sup>16</sup>

**Deutsches Elektronen-Synchrotron, Hamburg, Germany**

M. Aldaya Martin, T. Arndt, C. Asawatangtrakuldee, K. Beernaert, O. Behnke, U. Behrens, A. A. Bin Anuar, K. Borras<sup>17</sup>, A. Campbell, P. Connor, C. Contreras-Campana, F. Costanza, C. Diez Pardos, G. Dolinska, G. Eckerlin, D. Eckstein, T. Eichhorn, E. Eren, E. Gallo<sup>18</sup>, J. Garay Garcia, A. Geiser, A. Gizhko, J. M. Grados Luyando, P. Gunnellini, A. Harb, J. Hauk, M. Hempel<sup>19</sup>, H. Jung, A. Kalogeropoulos, O. Karacheban<sup>19</sup>, M. Kasemann, J. Keaveney, C. Kleinwort, I. Korol, D. Krücker, W. Lange, A. Lelek, J. Leonard, K. Lipka, A. Lobanov, W. Lohmann<sup>19</sup>, R. Mankel, I.-A. Melzer-Pellmann, A. B. Meyer, G. Mittag, J. Mnich, A. Mussgiller, E. Ntomari, D. Pitzl, R. Placakyte, A. Raspereza, B. Roland, M.Ö. Sahin, P. Saxena, T. Schoerner-Sadenius, C. Seitz, S. Spannagel, N. Stefaniuk, G. P. Van Onsem, R. Walsh, C. Wissing

**University of Hamburg, Hamburg, Germany**

V. Blobel, M. Centis Vignali, A. R. Draeger, T. Dreyer, E. Garutti, D. Gonzalez, J. Haller, M. Hoffmann, A. Junkes, R. Klanner, R. Kogler, N. Kovalchuk, T. Lapsien, T. Lenz, I. Marchesini, D. Marconi, M. Meyer, M. Niedziela, D. Nowatschin, F. Pantaleo<sup>16</sup>, T. Peiffer, A. Perieanu, J. Poehlsen, C. Sander, C. Scharf, P. Schleper, A. Schmidt, S. Schumann, J. Schwandt, H. Stadie, G. Steinbrück, F. M. Stober, M. Stöver, H. Tholen, D. Troendle, E. Usai, L. Vanelderen, A. Vanhoefer, B. Vormwald

**Institut für Experimentelle Kernphysik, Karlsruhe, Germany**

M. Akbiyik, C. Barth, S. Baur, C. Baus, J. Berger, E. Butz, R. Caspart, T. Chwalek, F. Colombo, W. De Boer, A. Dierlamm, S. Fink, B. Freund, R. Friese, M. Giffels, A. Gilbert, P. Goldenzweig, D. Haitz, F. Hartmann<sup>16</sup>, S. M. Heindl, U. Husemann, I. Katkov<sup>14</sup>, S. Kudella, P. Lobelle Pardo, H. Mildner, M. U. Mozer, Th. Müller, M. Plagge, G. Quast, K. Rabbertz, S. Röcker, F. Roscher, M. Schröder, I. Shvetsov, G. Sieber, H. J. Simonis, R. Ulrich, J. Wagner-Kuhr, S. Wayand, M. Weber, T. Weiler, S. Williamson, C. Wöhrmann, R. Wolf

**Institute of Nuclear and Particle Physics (INPP), NCSR Demokritos, Aghia Paraskevi, Greece**

G. Anagnostou, G. Daskalakis, T. Geralis, V. A. Giakoumopoulou, A. Kyriakis, D. Loukas, I. Topsis-Giotis

**National and Kapodistrian University of Athens, Athens, Greece**

S. Kesisoglou, A. Panagiotou, N. Saoulidou, E. Tziaferi

**University of Ioánnina, Ioannina, Greece**

I. Evangelou, G. Flouris, C. Foudas, P. Kokkas, N. Loukas, N. Manthos, I. Papadopoulos, E. Paradas

**MTA-ELTE Lendület CMS Particle and Nuclear Physics Group, Eötvös Loránd University, Budapest, Hungary**

N. Filipovic

**Wigner Research Centre for Physics, Budapest, Hungary**

G. Bencze, C. Hajdu, D. Horvath<sup>20</sup>, F. Sikler, V. Veszpremi, G. Vesztergombi<sup>21</sup>, A. J. Zsigmond

**Institute of Nuclear Research ATOMKI, Debrecen, Hungary**

N. Beni, S. Czellar, J. Karancsi<sup>22</sup>, A. Makovec, J. Molnar, Z. Szillasi

**University of Debrecen, Debrecen, Hungary**

M. Bartók<sup>21</sup>, P. Raics, Z. L. Trocsanyi, B. Ujvari

**National Institute of Science Education and Research, Bhubaneswar, India**

S. Bahinipati, S. Choudhury<sup>23</sup>, P. Mal, K. Mandal, A. Nayak<sup>24</sup>, D. K. Sahoo, N. Sahoo, S. K. Swain

**Panjab University, Chandigarh, India**

S. Bansal, S. B. Beri, V. Bhatnagar, R. Chawla, U. Bhawandeep, A. K. Kalsi, A. Kaur, M. Kaur, R. Kumar, P. Kumari, A. Mehta, M. Mittal, J. B. Singh, G. Walia

**University of Delhi, Delhi, India**

Ashok Kumar, A. Bhardwaj, B. C. Choudhary, R. B. Garg, S. Keshri, S. Malhotra, M. Naimuddin, N. Nishu, K. Ranjan, R. Sharma, V. Sharma

**Saha Institute of Nuclear Physics, Kolkata, India**

R. Bhattacharya, S. Bhattacharya, K. Chatterjee, S. Dey, S. Dutt, S. Dutta, S. Ghosh, N. Majumdar, A. Modak, K. Mondal, S. Mukhopadhyay, S. Nandan, A. Purohit, A. Roy, D. Roy, S. Roy Chowdhury, S. Sarkar, M. Sharan, S. Thakur

**Indian Institute of Technology Madras, Madras, India**

P. K. Behera

**Bhabha Atomic Research Centre, Mumbai, India**

R. Chudasama, D. Dutta, V. Jha, V. Kumar, A. K. Mohanty<sup>16</sup>, P. K. Netrakanti, L. M. Pant, P. Shukla, A. Topkar

**Tata Institute of Fundamental Research-A, Mumbai, India**

T. Aziz, S. Dugad, G. Kole, B. Mahakud, S. Mitra, G. B. Mohanty, B. Parida, N. Sur, B. Sutar

**Tata Institute of Fundamental Research-B, Mumbai, India**

S. Banerjee, S. Bhowmik<sup>25</sup>, R. K. Dewanjee, S. Ganguly, M. Guchait, Sa. Jain, S. Kumar, M. Maity<sup>25</sup>, G. Majumder, K. Mazumdar, T. Sarkar<sup>25</sup>, N. Wickramage<sup>26</sup>

**Indian Institute of Science Education and Research (IISER), Pune, India**

S. Chauhan, S. Dube, V. Hegde, A. Kapoor, K. Kothekar, S. Pandey, A. Rane, S. Sharma

**Institute for Research in Fundamental Sciences (IPM), Tehran, Iran**

H. Behnamian, S. Chenarani<sup>27</sup>, E. Eskandari Tadavani, S. M. Etesami<sup>27</sup>, A. Fahim<sup>28</sup>, M. Khakzad, M. Mohammadi Najafabadi, M. Naseri, S. Paktinat Mehdiabadi<sup>29</sup>, F. Rezaei Hosseinabadi, B. Safarzadeh<sup>30</sup>, M. Zeinali

**University College Dublin, Dublin, Ireland**

M. Felcini, M. Grunewald

**INFN Sezione di Bari<sup>a</sup>, Università di Bari<sup>b</sup>, Politecnico di Bari<sup>c</sup>, Bari, Italy**

M. Abbrescia<sup>a,b</sup>, C. Calabria<sup>a,b</sup>, C. Caputo<sup>a,b</sup>, A. Colaleo<sup>a</sup>, D. Creanza<sup>a,c</sup>, L. Cristella<sup>a,b</sup>, N. De Filippis<sup>a,c</sup>, M. De Palma<sup>a,b</sup>, L. Fiore<sup>a</sup>, G. Iaselli<sup>a,c</sup>, G. Maggi<sup>a,c</sup>, M. Maggi<sup>a</sup>, G. Miniello<sup>a,b</sup>, S. My<sup>a,b</sup>, S. Nuzzo<sup>a,b</sup>, A. Pompili<sup>a,b</sup>, G. Pugliese<sup>a,c</sup>, R. Radogna<sup>a,b</sup>, A. Ranieri<sup>a</sup>, G. Selvaggi<sup>a,b</sup>, L. Silvestris<sup>a,16</sup>, R. Venditti<sup>a,b</sup>, P. Verwilligen<sup>a</sup>

**INFN Sezione di Bologna<sup>a</sup>, Università di Bologna<sup>b</sup>, Bologna, Italy**

G. Abbiendi<sup>a</sup>, C. Battilana, D. Bonacorsi<sup>a,b</sup>, S. Braibant-Giacomelli<sup>a,b</sup>, L. Brigliadori<sup>a,b</sup>, R. Campanini<sup>a,b</sup>, P. Capiluppi<sup>a,b</sup>, A. Castro<sup>a,b</sup>, F. R. Cavallo<sup>a</sup>, S. S. Chhibra<sup>a,b</sup>, G. Codispoti<sup>a,b</sup>, M. Cuffiani<sup>a,b</sup>, G. M. Dallavalle<sup>a</sup>, F. Fabbri<sup>a</sup>, A. Fanfani<sup>a,b</sup>, D. Fasanella<sup>a,b</sup>, P. Giacomelli<sup>a</sup>, C. Grandi<sup>a</sup>, L. Guiducci<sup>a,b</sup>, S. Marcellini<sup>a</sup>, G. Masetti<sup>a</sup>, A. Montanari<sup>a</sup>, F. L. Navarria<sup>a,b</sup>, A. Perrotta<sup>a</sup>, A. M. Rossi<sup>a,b</sup>, T. Rovelli<sup>a,b</sup>, G. P. Siroli<sup>a,b</sup>, N. Tosi<sup>a,b,16</sup>

**INFN Sezione di Catania<sup>a</sup>, Università di Catania<sup>b</sup>, Catania, Italy**

S. Albergo<sup>a,b</sup>, S. Costa<sup>a,b</sup>, A. Di Mattia<sup>a</sup>, F. Giordano<sup>a,b</sup>, R. Potenza<sup>a,b</sup>, A. Tricomi<sup>a,b</sup>, C. Tuve<sup>a,b</sup>

**INFN Sezione di Firenze<sup>a</sup>, Università di Firenze<sup>b</sup>, Firenze, Italy**

G. Barbagli<sup>a</sup>, V. Ciulli<sup>a,b</sup>, C. Civinini<sup>a</sup>, R. D'Alessandro<sup>a,b</sup>, E. Focardi<sup>a,b</sup>, P. Lenzi<sup>a,b</sup>, M. Meschini<sup>a</sup>, S. Paoletti<sup>a</sup>, G. Sguazzoni<sup>a</sup>, L. Viliani<sup>a,b,16</sup>

**INFN Laboratori Nazionali di Frascati, Frascati, Italy**

L. Benussi, S. Bianco, F. Fabbri, D. Piccolo, F. Primavera<sup>16</sup>

**INFN Sezione di Genova<sup>a</sup>, Università di Genova<sup>b</sup>, Genova, Italy**

V. Calvelli<sup>a,b</sup>, F. Ferro<sup>a</sup>, M. Lo Vetere<sup>a,b</sup>, M. R. Monge<sup>a,b</sup>, E. Robutti<sup>a</sup>, S. Tosi<sup>a,b</sup>

**INFN Sezione di Milano-Bicocca<sup>a</sup>, Università di Milano-Bicocca<sup>b</sup>, Milano, Italy**

L. Brianza<sup>16</sup>, M. E. Dinardo<sup>a,b</sup>, S. Fiorendi<sup>a,b,16</sup>, S. Gennai<sup>a</sup>, A. Ghezzi<sup>a,b</sup>, P. Govoni<sup>a,b</sup>, M. Malberti, S. Malvezzi<sup>a</sup>, R. A. Manzoni<sup>a,b,16</sup>, D. Menasce<sup>a</sup>, L. Moroni<sup>a</sup>, M. Paganoni<sup>a,b</sup>, D. Pedrini<sup>a</sup>, S. Pigazzini, S. Ragazzi<sup>a,b</sup>, T. Tabarelli de Fatis<sup>a,b</sup>

**INFN Sezione di Napoli<sup>a</sup>, Università di Napoli 'Federico II'<sup>b</sup>, Napoli, Italy, Università della Basilicata<sup>c</sup>, Potenza, Italy, Università G. Marconi<sup>d</sup>, Rome, Italy**

S. Buontempo<sup>a</sup>, N. Cavallo<sup>a,c</sup>, G. De Nardo, S. Di Guida<sup>a,d,16</sup>, M. Esposito<sup>a,b</sup>, F. Fabozzi<sup>a,c</sup>, F. Fienga<sup>a,b</sup>, A. O. M. Iorio<sup>a,b</sup>, G. Lanza<sup>a</sup>, L. Lista<sup>a</sup>, S. Meola<sup>a,d,16</sup>, P. Paolucci<sup>a,16</sup>, C. Sciacca<sup>a,b</sup>, F. Thyssen

**INFN Sezione di Padova<sup>a</sup>, Università di Padova<sup>b</sup>, Padova, Italy, Università di Trento<sup>c</sup>, Trento, Italy**

P. Azzi<sup>a,16</sup>, N. Bacchetta<sup>a</sup>, L. Benato<sup>a,b</sup>, D. Bisello<sup>a,b</sup>, A. Boletti<sup>a,b</sup>, R. Carlin<sup>a,b</sup>, A. Carvalho Antunes De Oliveira<sup>a,b</sup>, P. Checchia<sup>a</sup>, M. Dall'Osso<sup>a,b</sup>, P. De Castro Manzano<sup>a</sup>, T. Dorigo<sup>a</sup>, U. Dosselli<sup>a</sup>, F. Gasparini<sup>a,b</sup>, U. Gasparini<sup>a,b</sup>, A. Gozzelino<sup>a</sup>, S. Lacaprara<sup>a</sup>, M. Margoni<sup>a,b</sup>, A. T. Meneguzzo<sup>a,b</sup>, J. Pazzini<sup>a,b</sup>, N. Pozzobon<sup>a,b</sup>, P. Ronchese<sup>a,b</sup>, F. Simonetto<sup>a,b</sup>, E. Torassa<sup>a</sup>, M. Zanetti, P. Zotto<sup>a,b</sup>, G. Zumerle<sup>a,b</sup>

**INFN Sezione di Pavia<sup>a</sup>, Università di Pavia<sup>b</sup>, Pavia, Italy**

A. Braghieri<sup>a</sup>, A. Magnani<sup>a,b</sup>, P. Montagna<sup>a,b</sup>, S. P. Ratti<sup>a,b</sup>, V. Re<sup>a</sup>, C. Riccardi<sup>a,b</sup>, P. Salvini<sup>a</sup>, I. Vai<sup>a,b</sup>, P. Vitulo<sup>a,b</sup>

**INFN Sezione di Perugia<sup>a</sup>, Università di Perugia<sup>b</sup>, Perugia, Italy**

L. Alunni Solestizi<sup>a,b</sup>, G. M. Bilei<sup>a</sup>, D. Ciangottini<sup>a,b</sup>, L. Fanò<sup>a,b</sup>, P. Lariccia<sup>a,b</sup>, R. Leonardi<sup>a,b</sup>, G. Mantovani<sup>a,b</sup>, M. Menichelli<sup>a</sup>, A. Saha<sup>a</sup>, A. Santocchia<sup>a,b</sup>

**INFN Sezione di Pisa<sup>a</sup>, Università di Pisa<sup>b</sup>, Scuola Normale Superiore di Pisa<sup>c</sup>, Pisa, Italy**

K. Androsov<sup>a,31</sup>, P. Azzurri<sup>a,16</sup>, G. Bagliesi<sup>a</sup>, J. Bernardini<sup>a</sup>, T. Boccali<sup>a</sup>, R. Castaldi<sup>a</sup>, M. A. Ciocci<sup>a,31</sup>, R. Dell'Orso<sup>a</sup>, S. Donato<sup>a,c</sup>, G. Fedi, A. Giassi<sup>a</sup>, M. T. Grippo<sup>a,31</sup>, F. Ligabue<sup>a,c</sup>, T. Lomtadze<sup>a</sup>, L. Martini<sup>a,b</sup>, A. Messineo<sup>a,b</sup>, F. Palla<sup>a</sup>, A. Rizzi<sup>a,b</sup>, A. Savoy-Navarro<sup>a,32</sup>, P. Spagnolo<sup>a</sup>, R. Tenchini<sup>a</sup>, G. Tonelli<sup>a,b</sup>, A. Venturi<sup>a</sup>, P. G. Verdini<sup>a</sup>

**INFN Sezione di Roma<sup>a</sup>, Università di Roma<sup>b</sup>, Rome, Italy**

L. Barone<sup>a,b</sup>, F. Cavallari<sup>a</sup>, M. Cipriani<sup>a,b</sup>, D. Del Re<sup>a,b,16</sup>, M. Diemoz<sup>a</sup>, S. Gelli<sup>a,b</sup>, E. Longo<sup>a,b</sup>, F. Margaroli<sup>a,b</sup>, B. Marzocchi<sup>a,b</sup>, P. Meridiani<sup>a</sup>, G. Organtini<sup>a,b</sup>, R. Paramatti<sup>a</sup>, F. Preiato<sup>a,b</sup>, S. Rahatlou<sup>a,b</sup>, C. Rovelli<sup>a</sup>, F. Santanastasio<sup>a,b</sup>



**INFN Sezione di Torino<sup>a</sup>, Università di Torino<sup>b</sup>, Torino, Italy, Università del Piemonte Orientale<sup>c</sup>, Novara, Italy**  
 N. Amapane<sup>a,b</sup>, R. Arcidiacono<sup>a,c,16</sup>, S. Argiro<sup>a,b</sup>, M. Arneodo<sup>a,c</sup>, N. Bartosik<sup>a</sup>, R. Bellan<sup>a,b</sup>, C. Biino<sup>a</sup>, N. Cartiglia<sup>a</sup>,  
 F. Cenna<sup>a,b</sup>, M. Costa<sup>a,b</sup>, R. Covarelli<sup>a,b</sup>, A. Degano<sup>a,b</sup>, N. Demaria<sup>a</sup>, L. Finco<sup>a,b</sup>, B. Kiani<sup>a,b</sup>, C. Mariotti<sup>a</sup>, S. Maselli<sup>a</sup>,  
 E. Migliore<sup>a,b</sup>, V. Monaco<sup>a,b</sup>, E. Monteil<sup>a,b</sup>, M. Monteno<sup>a</sup>, M. M. Obertino<sup>a,b</sup>, L. Pacher<sup>a,b</sup>, N. Pastrone<sup>a</sup>, M. Pelliccioni<sup>a</sup>,  
 G. L. Pinna Angioni<sup>a,b</sup>, F. Ravera<sup>a,b</sup>, A. Romero<sup>a,b</sup>, M. Ruspa<sup>a,c</sup>, R. Sacchi<sup>a,b</sup>, K. Shchelina<sup>a,b</sup>, V. Sola<sup>a</sup>, A. Solano<sup>a,b</sup>,  
 A. Staiano<sup>a</sup>, P. Traczyk<sup>a,b</sup>

**INFN Sezione di Trieste<sup>a</sup>, Università di Trieste<sup>b</sup>, Trieste, Italy**  
 S. Belforte<sup>a</sup>, M. Casarsa<sup>a</sup>, F. Cossutti<sup>a</sup>, G. Della Ricca<sup>a,b</sup>, A. Zanetti<sup>a</sup>

**Kyungpook National University, Daegu, Korea**

D. H. Kim, G. N. Kim, M. S. Kim, S. Lee, S. W. Lee, Y. D. Oh, S. Sekmen, D. C. Son, Y. C. Yang

**Chonbuk National University, Jeonju, Korea**

A. Lee

**Chonnam National University, Institute for Universe and Elementary Particles, Kwangju, Korea**

H. Kim, D. H. Moon

**Hanyang University, Seoul, Korea**

J. A. Brochero Cifuentes, T. J. Kim

**Korea University, Seoul, Korea**

S. Cho, S. Choi, Y. Go, D. Gyun, S. Ha, B. Hong, Y. Jo, Y. Kim, B. Lee, K. Lee, K. S. Lee, S. Lee, J. Lim, S. K. Park,  
 Y. Roh

**Seoul National University, Seoul, Korea**

J. Almond, J. Kim, H. Lee, S. B. Oh, B. C. Radburn-Smith, S. H. Seo, U. K. Yang, H. D. Yoo, G. B. Yu

**University of Seoul, Seoul, Korea**

M. Choi, H. Kim, J. H. Kim, J. S. H. Lee, I. C. Park, G. Ryu, M. S. Ryu

**Sungkyunkwan University, Suwon, Korea**

Y. Choi, J. Goh, C. Hwang, J. Lee, I. Yu

**Vilnius University, Vilnius, Lithuania**

V. Dudenas, A. Juodagalvis, J. Vaitkus

**National Centre for Particle Physics, Universiti Malaya, Kuala Lumpur, Malaysia**

I. Ahmed, Z. A. Ibrahim, J. R. Komaragiri, M. A. B. Md Ali<sup>33</sup>, F. Mohamad Idris<sup>34</sup>, W. A. T. Wan Abdullah, M. N. Yusli,  
 Z. Zolkapli

**Centro de Investigacion y de Estudios Avanzados del IPN, Mexico City, Mexico**

H. Castilla-Valdez, E. De La Cruz-Burelo, I. Heredia-De La Cruz<sup>35</sup>, A. Hernandez-Almada, R. Lopez-Fernandez,  
 R. Magaña Villalba, J. Mejia Guisao, A. Sanchez-Hernandez

**Universidad Iberoamericana, Mexico City, Mexico**

S. Carrillo Moreno, C. Oropeza Barrera, F. Vazquez Valencia

**Benemerita Universidad Autonoma de Puebla, Puebla, Mexico**

S. Carpinteyro, I. Pedraza, H. A. Salazar Ibarguen, C. Uribe Estrada

**Universidad Autónoma de San Luis Potosí, San Luis Potosí, Mexico**

A. Morelos Pineda

**University of Auckland, Auckland, New Zealand**

D. Krofcheck

**University of Canterbury, Christchurch, New Zealand**

P. H. Butler

**National Centre for Physics, Quaid-I-Azam University, Islamabad, Pakistan**

A. Ahmad, M. Ahmad, Q. Hassan, H. R. Hoorani, W. A. Khan, A. Saddique, M. A. Shah, M. Shoaib, M. Waqas

**National Centre for Nuclear Research, Swierk, Poland**

H. Bialkowska, M. Bluj, B. Boimska, T. Frueboes, M. Górski, M. Kazana, K. Nawrocki, K. Romanowska-Rybinska, M. Szleper, P. Zalewski

**Institute of Experimental Physics, Faculty of Physics, University of Warsaw, Warsaw, Poland**

K. Bunkowski, A. Byszuk<sup>36</sup>, K. Doroba, A. Kalinowski, M. Konecki, J. Krolikowski, M. Misiura, M. Olszewski, M. Walczak

**Laboratório de Instrumentação e Física Experimental de Partículas, Lisboa, Portugal**

P. Bargassa, C. Beirão Da Cruz E Silva, B. Calpas, A. Di Francesco, P. Faccioli, P. G. Ferreira Parracho, M. Gallinaro, J. Hollar, N. Leonardo, L. Lloret Iglesias, M. V. Nemallapudi, J. Rodrigues Antunes, J. Seixas, O. Toldaiev, D. Vadrucio, J. Varela, P. Vischia

**Joint Institute for Nuclear Research, Dubna, Russia**

S. Afanasiev, P. Bunin, M. Gavrilenko, I. Golutvin, I. Gorbunov, A. Kamenev, V. Karjavin, A. Lanev, A. Malakhov, V. Matveev<sup>37,38</sup>, V. Palichik, V. Perelygin, S. Shmatov, S. Shulha, N. Skatchkov, V. Smirnov, N. Voytishin, A. Zarubin

**Petersburg Nuclear Physics Institute, Gatchina, St. Petersburg, Russia**

L. Chtchipounov, V. Golovtsov, Y. Ivanov, V. Kim<sup>39</sup>, E. Kuznetsova<sup>40</sup>, V. Murzin, V. Oreshkin, V. Sulimov, A. Vorobyev

**Institute for Nuclear Research, Moscow, Russia**

Yu. Andreev, A. Dermenev, S. Gninenko, N. Golubev, A. Karneyeu, M. Kirsanov, N. Krasnikov, A. Pashenkov, D. Tlisov, A. Toropin

**Institute for Theoretical and Experimental Physics, Moscow, Russia**

V. Epshteyn, V. Gavrilov, N. Lychkovskaya, V. Popov, I. Pozdnyakov, G. Safronov, A. Spiridonov, M. Toms, E. Vlasov, A. Zhokin

**Moscow Institute of Physics and Technology, Dolgoprudny, Russia**

A. Bylinkin<sup>38</sup>

**National Research Nuclear University ‘Moscow Engineering Physics Institute’ (MEPhI), Moscow, Russia**

R. Chistov<sup>41</sup>, S. Polikarpov, V. Rusinov

**P.N. Lebedev Physical Institute, Moscow, Russia**

V. Andreev, M. Azarkin<sup>38</sup>, I. Dremin<sup>38</sup>, M. Kirakosyan, A. Leonidov<sup>38</sup>, A. Terkulov

**Skobeltsyn Institute of Nuclear Physics, Lomonosov Moscow State University, Moscow, Russia**

A. Baskakov, A. Belyaev, E. Boos, A. Demiyarov, A. Ershov, A. Gribushin, O. Kodolova, V. Korotkikh, I. Lokhtin, I. Miagkov, S. Obraztsov, S. Petrushanko, V. Savrin, A. Snigirev, I. Vardanyan

**Novosibirsk State University (NSU), Novosibirsk, Russia**

V. Blinov<sup>42</sup>, Y. Skovpen<sup>42</sup>, D. Shtol<sup>42</sup>

**State Research Center of Russian Federation, Institute for High Energy Physics, Protvino, Russia**

I. Azhgirey, I. Bayshev, S. Bitioukov, D. Elumakhov, V. Kachanov, A. Kalinin, D. Konstantinov, V. Krychkin, V. Petrov, R. Ryutin, A. Sobol, S. Troshin, N. Tyurin, A. Uzunian, A. Volkov

**University of Belgrade, Faculty of Physics and Vinca Institute of Nuclear Sciences, Belgrade, Serbia**

P. Adzic<sup>43</sup>, P. Cirkovic, D. Devetak, M. Dordevic, J. Milosevic, V. Rekovic

**Centro de Investigaciones Energéticas Medioambientales y Tecnológicas (CIEMAT), Madrid, Spain**

J. Alcaraz Maestre, M. Barrio Luna, E. Calvo, M. Cerrada, M. Chamizo Llatas, N. Colino, B. De La Cruz, A. Delgado Peris, A. Escalante Del Valle, C. Fernandez Bedoya, J. P. Fernández Ramos, J. Flix, M. C. Fouz, P. Garcia-Abia, O. Gonzalez Lopez, S. Goy Lopez, J. M. Hernandez, M. I. Josa, E. Navarro De Martino, A. Pérez-Calero Yzquierdo, J. Puerta Pelayo, A. Quintario Olmeda, I. Redondo, L. Romero, M. S. Soares

**Universidad Autónoma de Madrid, Madrid, Spain**

J. F. de Trocóniz, M. Missiroli, D. Moran

**Universidad de Oviedo, Oviedo, Spain**

J. Cuevas, J. Fernandez Menendez, I. Gonzalez Caballero, J. R. González Fernández, E. Palencia Cortezon, S. Sanchez Cruz, I. Suárez Andrés, J. M. Vizan Garcia

**Instituto de Física de Cantabria (IFCA), CSIC-Universidad de Cantabria, Santander, Spain**

I. J. Cabrillo, A. Calderon, J. R. Castiñeiras De Saa, E. Curras, M. Fernandez, J. Garcia-Ferrero, G. Gomez, A. Lopez Virto, J. Marco, C. Martinez Rivero, F. Matorras, J. Piedra Gomez, T. Rodrigo, A. Ruiz-Jimeno, L. Scodellaro, N. Trevisani, I. Vila, R. Vilar Cortabitarte

**CERN, European Organization for Nuclear Research, Geneva, Switzerland**

D. Abbaneo, E. Auffray, G. Auzinger, M. Bachtis, P. Baillon, A. H. Ball, D. Barney, P. Bloch, A. Bocci, A. Bonato, C. Botta, T. Camporesi, R. Castello, M. Cepeda, G. Cerminara, M. D'Alfonso, D. d'Enterria, A. Dabrowski, V. Daponte, A. David, M. De Gruttola, A. De Roeck, E. Di Marco<sup>44</sup>, M. Dobson, B. Dorney, T. du Pree, D. Duggan, M. Dünser, N. Dupont, A. Elliott-Peisert, S. Fartoukh, G. Franzoni, J. Fulcher, W. Funk, D. Gigi, K. Gill, M. Girone, F. Glege, D. Gulhan, S. Gundacker, M. Guthoff, J. Hammer, P. Harris, J. Hegeman, V. Innocente, P. Janot, J. Kieseler, H. Kirschenmann, V. Knünz, A. Kornmayer<sup>16</sup>, M. J. Kortelainen, K. Kousouris, M. Krammer<sup>1</sup>, C. Lange, P. Lecoq, C. Lourenço, M. T. Lucchini, L. Malgeri, M. Mannelli, A. Martelli, F. Meijers, J. A. Merlin, S. Mersi, E. Meschi, P. Milenovic<sup>45</sup>, F. Moortgat, S. Morovic, M. Mulders, H. Neugebauer, S. Orfanelli, L. Orsini, L. Pape, E. Perez, M. Peruzzi, A. Petrilli, G. Petrucciani, A. Pfeiffer, M. Pierini, A. Racz, T. Reis, G. Rolandi<sup>46</sup>, M. Rovere, M. Ruan, H. Sakulin, J. B. Sauvan, C. Schäfer, C. Schwick, M. Seidel, A. Sharma, P. Silva, P. Sphicas<sup>47</sup>, J. Steggemann, M. Stoye, Y. Takahashi, M. Tosi, D. Treille, A. Triossi, A. Tsirou, V. Veckalns<sup>48</sup>, G. I. Veres<sup>21</sup>, M. Verweij, N. Wardle, H. K. Wöhri, A. Zagozdinska<sup>36</sup>, W. D. Zeuner

**Paul Scherrer Institut, Villigen, Switzerland**

W. Bertl, K. Deiters, W. Erdmann, R. Horisberger, Q. Ingram, H. C. Kaestli, D. Kotlinski, U. Langenegger, T. Rohe

**Institute for Particle Physics, ETH Zurich, Zurich, Switzerland**

F. Bachmair, L. Bäni, L. Bianchini, B. Casal, G. Dissertori, M. Dittmar, M. Donegà, C. Grab, C. Heidegger, D. Hits, J. Hoss, G. Kasieczka, P. Lecomte<sup>†</sup>, W. Lustermann, B. Mangano, M. Marionneau, P. Martinez Ruiz del Arbol, M. Masciovecchio, M. T. Meinhard, D. Meister, F. Micheli, P. Musella, F. Nessi-Tedaldi, F. Pandolfi, J. Pata, F. Pauss, G. Perrin, L. Perrozzi, M. Quittnat, M. Rossini, M. Schönenberger, A. Starodumov<sup>49</sup>, V. R. Tavolaro, K. Theofilatos, R. Wallny

**Universität Zürich, Zurich, Switzerland**

T. K. Aarrestad, C. Amsler<sup>50</sup>, L. Caminada, M. F. Canelli, A. De Cosa, C. Galloni, A. Hinzmann, T. Hreus, B. Kilminster, J. Ngadiuba, D. Pinna, G. Rauco, P. Robmann, D. Salerno, Y. Yang, A. Zucchetta

**National Central University, Chung-Li, Taiwan**

V. Candelise, T. H. Doan, Sh. Jain, R. Khurana, M. Konyushikhin, C. M. Kuo, W. Lin, Y. J. Lu, A. Pozdnyakov, S. S. Yu

**National Taiwan University (NTU), Taipei, Taiwan**

Arun Kumar, P. Chang, Y. H. Chang, Y. W. Chang, Y. Chao, K. F. Chen, P. H. Chen, C. Dietz, F. Fiori, W.-S. Hou, Y. Hsiung, Y. F. Liu, R.-S. Lu, M. Miñano Moya, E. Paganis, A. Psallidas, J. F. Tsai, Y. M. Tzeng

**Chulalongkorn University, Faculty of Science, Department of Physics, Bangkok, Thailand**

B. Asavapibhop, G. Singh, N. Srimanobhas, N. Suwonjandee

**Cukurova University, Adana, Turkey**

A. Adiguzel, S. Cerci<sup>51</sup>, S. Damarseckin, Z. S. Demiroglu, C. Dozen, I. Dumanoglu, S. Girgis, G. Gokbulut, Y. Guler, I. Hos<sup>52</sup>, E. E. Kangal<sup>53</sup>, O. Kara, A. Kayis Topaksu, U. Kiminsu, M. Oglakci, G. Onengut<sup>54</sup>, K. Ozdemir<sup>55</sup>, D. Sunar Cerci<sup>51</sup>, B. Tali<sup>51</sup>, S. Turkcapar, I. S. Zorbakir, C. Zorbilmez

**Middle East Technical University, Physics Department, Ankara, Turkey**

B. Bilin, S. Bilmis, B. Isildak<sup>56</sup>, G. Karapinar<sup>57</sup>, M. Yalvac, M. Zeyrek

**Bogazici University, Istanbul, Turkey**

E. Gülmez, M. Kaya<sup>58</sup>, O. Kaya<sup>59</sup>, E. A. Yetkin<sup>60</sup>, T. Yetkin<sup>61</sup>

**Istanbul Technical University, Istanbul, Turkey**

A. Cakir, K. Cankocak, S. Sen<sup>62</sup>

**Institute for Scintillation Materials of National Academy of Science of Ukraine, Kharkov, Ukraine**

B. Grynyov

**National Scientific Center, Kharkov Institute of Physics and Technology, Kharkov, Ukraine**

L. Levchuk, P. Sorokin

**University of Bristol, Bristol, UK**

R. Aggleton, F. Ball, L. Beck, J. J. Brooke, D. Burns, E. Clement, D. Cussans, H. Flacher, J. Goldstein, M. Grimes, G. P. Heath, H. F. Heath, J. Jacob, L. Kreczko, C. Lucas, D. M. Newbold<sup>63</sup>, S. Paramesvaran, A. Poll, T. Sakuma, S. Seif El Nasr-storey, D. Smith, V. J. Smith

**Rutherford Appleton Laboratory, Didcot, UK**

A. Belyaev<sup>64</sup>, C. Brew, R. M. Brown, L. Calligaris, D. Cieri, D. J. A. Cockerill, J. A. Coughlan, K. Harder, S. Harper, E. Olaiya, D. Petyt, C. H. Shepherd-Themistocleous, A. Thea, I. R. Tomalin, T. Williams

**Imperial College, London, UK**

M. Baber, R. Bainbridge, O. Buchmuller, A. Bundock, D. Burton, S. Casasso, M. Citron, D. Colling, L. Corpe, P. Dauncey, G. Davies, A. De Wit, M. Della Negra, R. Di Maria, P. Dunne, A. Elwood, D. Futyan, Y. Haddad, G. Hall, G. Iles, T. James, R. Lane, C. Laner, R. Lucas<sup>65</sup>, L. Lyons, A.-M. Magnan, S. Malik, L. Mastrolorenzo, J. Nash, A. Nikitenko<sup>49</sup>, J. Pela, B. Penning, M. Pesaresi, D. M. Raymond, A. Richards, A. Rose, C. Seez, S. Summers, A. Tapper, K. Uchida, M. Vazquez Acosta<sup>65</sup>, T. Virdee<sup>16</sup>, J. Wright, S. C. Zenz

**Brunel University, Uxbridge, UK**

J. E. Cole, P. R. Hobson, A. Khan, P. Kyberd, D. Leslie, I. D. Reid, P. Symonds, L. Teodorescu, M. Turner

**Baylor University, Waco, USA**

A. Borzou, K. Call, J. Dittmann, K. Hatakeyama, H. Liu, N. Pastika

**The University of Alabama, Tuscaloosa, USA**

S. I. Cooper, C. Henderson, P. Rumerio, C. West

**Boston University, Boston, USA**

D. Arcaro, A. Avetisyan, T. Bose, D. Gastler, D. Rankin, C. Richardson, J. Rohlf, L. Sulak, D. Zou

**Brown University, Providence, USA**

G. Benelli, E. Berry, D. Cutts, A. Garabedian, J. Hakala, U. Heintz, J. M. Hogan, O. Jesus, K. H. M. Kwok, E. Laird, G. Landsberg, Z. Mao, M. Narain, S. Piperov, S. Sagir, E. Spencer, R. Syarif

**University of California, Davis, Davis, USA**

R. Breedon, G. Breto, D. Burns, M. Calderon De La Barca Sanchez, S. Chauhan, M. Chertok, J. Conway, R. Conway, P. T. Cox, R. Erbacher, C. Flores, G. Funk, M. Gardner, W. Ko, R. Lander, C. Mclean, M. Mulhearn, D. Pellett, J. Pilot, S. Shalhout, J. Smith, M. Squires, D. Stolp, M. Tripathi

**University of California, Los Angeles, USA**

C. Bravo, R. Cousins, A. Dasgupta, P. Everaerts, A. Florent, J. Hauser, M. Ignatenko, N. Mccoll, D. Saltzberg, C. Schnaible, E. Takasugi, V. Valuev, M. Weber

**University of California, Riverside, Riverside, USA**

K. Burt, R. Clare, J. Ellison, J. W. Gary, S. M. A. Ghiasi Shirazi, G. Hanson, J. Heilman, P. Jandir, E. Kennedy, F. Lacroix, O. R. Long, M. Olmedo Negrete, M. I. Paneva, A. Shrinivas, W. Si, H. Wei, S. Wimpenny, B. R. Yates

**University of California, San Diego, La Jolla, USA**

J. G. Branson, G. B. Cerati, S. Cittolin, M. Derdzinski, A. Holzner, D. Klein, V. Krutelyov, J. Letts, I. Macneill, D. Olivito, S. Padhi, M. Pieri, M. Sani, V. Sharma, S. Simon, M. Tadel, A. Vartak, S. Wasserbaech<sup>66</sup>, C. Welke, J. Wood, F. Würthwein, A. Yagil, G. Zevi Della Porta

**Santa Barbara-Department of Physics, University of California, Santa Barbara, USA**

N. Amin, R. Bhan dari, J. Bradmiller-Feld, C. Campagnari, A. Dishaw, V. Dutta, M. Franco Sevilla, C. George, F. Golf, L. Gouskos, J. Gran, R. Heller, J. Incandela, S. D. Mullin, A. Ovcharova, H. Qu, J. Richman, D. Stuart, I. Suarez, J. Yoo

**California Institute of Technology, Pasadena, USA**

D. Anderson, A. Apresyan, J. Bendavid, A. Bornheim, J. Bunn, Y. Chen, J. Duarte, J. M. Lawhorn, A. Mott, H. B. Newman, C. Pena, M. Spiropulu, J. R. Vlimant, S. Xie, R. Y. Zhu

**Carnegie Mellon University, Pittsburgh, USA**

M. B. Andrews, V. Azzolini, T. Ferguson, M. Paulini, J. Russ, M. Sun, H. Vogel, I. Vorobiev, M. Weinberg

**University of Colorado Boulder, Boulder, USA**

J. P. Cumalat, W. T. Ford, F. Jensen, A. Johnson, M. Krohn, T. Mulholland, K. Stenson, S. R. Wagner

**Cornell University, Ithaca, USA**

J. Alexander, J. Chaves, J. Chu, S. Dittmer, K. Mcdermott, N. Mirman, G. Nicolas Kaufman, J. R. Patterson, A. Rinkevicius, A. Ryd, L. Skinnari, L. Soffi, S. M. Tan, Z. Tao, J. Thom, J. Tucker, P. Wittich, M. Zientek

**Fairfield University, Fairfield, USA**

D. Winn

**Fermi National Accelerator Laboratory, Batavia, USA**

S. Abdullin, M. Albrow, G. Apollinari, S. Banerjee, L. A. T. Bauerdick, A. Beretvas, J. Berryhill, P. C. Bhat, G. Bolla, K. Burkett, J. N. Butler, H. W. K. Cheung, F. Chlebana, S. Cihangir<sup>†</sup>, M. Cremonesi, V. D. Elvira, I. Fisk, J. Freeman, E. Gottschalk, L. Gray, D. Green, S. Grünendahl, O. Gutsche, D. Hare, R. M. Harris, S. Hasegawa, J. Hirschauer, Z. Hu, B. Jayatilaka, S. Jindariani, M. Johnson, U. Joshi, B. Klima, B. Kreis, S. Lammel, J. Linacre, D. Lincoln, R. Lipton, T. Liu, R. Lopes De Sá, J. Lykken, K. Maeshima, N. Magini, J. M. Marraffino, S. Maruyama, D. Mason, P. McBride, P. Merkel, S. Mrenna, S. Nahn, C. Newman-Holmes<sup>†</sup>, V. O'Dell, K. Pedro, O. Prokofyev, G. Rakness, L. Ristori, E. Sexton-Kennedy, A. Soha, W. J. Spalding, L. Spiegel, S. Stoynev, N. Strobbe, L. Taylor, S. Tkaczyk, N. V. Tran, L. Uplegger, E. W. Vaandering, C. Vernieri, M. Verzocchi, R. Vidal, M. Wang, H. A. Weber, A. Whitbeck, Y. Wu

**University of Florida, Gainesville, USA**

D. Acosta, P. Avery, P. Bortignon, D. Bourilkov, A. Brinkerhoff, A. Carnes, M. Carver, D. Curry, S. Das, R. D. Field, I. K. Furic, J. Konigsberg, A. Korytov, J. F. Low, P. Ma, K. Matchev, H. Mei, G. Mitselmakher, D. Rank, L. Shchutka, D. Sperka, L. Thomas, J. Wang, S. Wang, J. Yelton

**Florida International University, Miami, USA**

S. Linn, P. Markowitz, G. Martinez, J. L. Rodriguez

**Florida State University, Tallahassee, USA**

A. Ackert, J. R. Adams, T. Adams, A. Askew, S. Bein, B. Diamond, S. Hagopian, V. Hagopian, K. F. Johnson, A. Khatiwada, H. Prosper, A. Santra, R. Yohay

**Florida Institute of Technology, Melbourne, USA**

M. M. Baarmand, V. Bhopatkar, S. Colafranceschi, M. Hohlmann, D. Noonan, T. Roy, F. Yumiceva

**University of Illinois at Chicago (UIC), Chicago, USA**

M. R. Adams, L. Apanasevich, D. Berry, R. R. Betts, I. Bucinskaite, R. Cavanaugh, O. Evdokimov, L. Gauthier, C. E. Gerber, D. J. Hofman, K. Jung, P. Kurt, C. O'Brien, I. D. Sandoval Gonzalez, P. Turner, N. Varelas, H. Wang, Z. Wu, M. Zakaria, J. Zhang



**The University of Iowa, Iowa City, USA**

B. Bilki<sup>67</sup>, W. Clarida, K. Dilsiz, S. Durgut, R. P. Gandrajula, M. Haytmyradov, V. Khristenko, J.-P. Merlo, H. Mermerkaya<sup>68</sup>, A. Mestvirishvili, A. Moeller, J. Nachtman, H. Ogul, Y. Onel, F. Ozok<sup>69</sup>, A. Penzo, C. Snyder, E. Tiras, J. Wetzel, K. Yi

**Johns Hopkins University, Baltimore, USA**

I. Anderson, B. Blumenfeld, A. Cocoros, N. Eminizer, D. Fehling, L. Feng, A. V. Gritsan, P. Maksimovic, C. Martin, M. Osherson, J. Roskes, U. Sarica, M. Swartz, M. Xiao, Y. Xin, C. You

**The University of Kansas, Lawrence, USA**

A. Al-bataineh, P. Baringer, A. Bean, S. Boren, J. Bowen, C. Bruner, J. Castle, L. Forthomme, R. P. Kenny III, S. Khalil, A. Kropivnitskaya, D. Majumder, W. Mcbrayer, M. Murray, S. Sanders, R. Stringer, J. D. Tapia Takaki, Q. Wang

**Kansas State University, Manhattan, USA**

A. Ivanov, K. Kaadze, Y. Maravin, A. Mohammadi, L. K. Saini, N. Skhirtladze, S. Toda

**Lawrence Livermore National Laboratory, Livermore, USA**

F. Rebasoo, D. Wright

**University of Maryland, College Park, USA**

C. Anelli, A. Baden, O. Baron, A. Belloni, B. Calvert, S. C. Eno, C. Ferraioli, J. A. Gomez, N. J. Hadley, S. Jabeen, R. G. Kellogg, T. Kolberg, J. Kunkle, Y. Lu, A. C. Mignerey, F. Ricci-Tam, Y. H. Shin, A. Skuja, M. B. Tonjes, S. C. Tonwar

**Massachusetts Institute of Technology, Cambridge, USA**

D. Abercrombie, B. Allen, A. Apyan, R. Barbieri, A. Baty, R. Bi, K. Bierwagen, S. Brandt, W. Busza, I. A. Cali, Z. Demiragli, L. Di Matteo, G. Gomez Ceballos, M. Goncharov, D. Hsu, Y. Iiyama, G. M. Innocenti, M. Klute, D. Kovalskyi, K. Krajczar, Y. S. Lai, Y.-J. Lee, A. Levin, P. D. Luckey, B. Maier, A. C. Marini, C. McGinn, C. Mironov, S. Narayanan, X. Niu, C. Paus, C. Roland, G. Roland, J. Salfeld-Nebgen, G. S. F. Stephans, K. Sumorok, K. Tatar, M. Varma, D. Velicanu, J. Veverka, J. Wang, T. W. Wang, B. Wyslouch, M. Yang, V. Zhukova

**University of Minnesota, Minneapolis, USA**

A. C. Benvenuti, R. M. Chatterjee, A. Evans, A. Finkel, A. Gude, P. Hansen, S. Kalafut, S. C. Kao, Y. Kubota, Z. Lesko, J. Mans, S. Nourbakhsh, N. Ruckstuhl, R. Rusack, N. Tambe, J. Turkewitz

**University of Mississippi, Oxford, USA**

J. G. Acosta, S. Oliveros

**University of Nebraska-Lincoln, Lincoln, USA**

E. Avdeeva, R. Bartek<sup>70</sup>, K. Bloom, D. R. Claes, A. Dominguez<sup>70</sup>, C. Fangmeier, R. Gonzalez Suarez, R. Kamalieddin, I. Kravchenko, A. Malta Rodrigues, F. Meier, J. Monroy, J. E. Siado, G. R. Snow, B. Stieger

**State University of New York at Buffalo, Buffalo, USA**

M. Alyari, J. Dolen, J. George, A. Godshalk, C. Harrington, I. Iashvili, J. Kaisen, A. Kharchilava, A. Kumar, A. Parker, S. Rappoccio, B. Roozbahani

**Northeastern University, Boston, USA**

G. Alverson, E. Barberis, A. Hortiangtham, A. Massironi, D. M. Morse, D. Nash, T. Orimoto, R. Teixeira De Lima, D. Trocino, R.-J. Wang, D. Wood

**Northwestern University, Evanston, USA**

S. Bhattacharya, O. Charaf, K. A. Hahn, A. Kubik, A. Kumar, N. Mucia, N. Odell, B. Pollack, M. H. Schmitt, K. Sung, M. Trovato, M. Velasco

**University of Notre Dame, Notre Dame, USA**

N. Dev, M. Hildreth, K. Hurtado Anampa, C. Jessop, D. J. Karmgard, N. Kellams, K. Lannon, N. Marinelli, F. Meng, C. Mueller, Y. Musienko<sup>37</sup>, M. Planer, A. Reinsvold, R. Ruchti, G. Smith, S. Taroni, M. Wayne, M. Wolf, A. Woodard

**The Ohio State University, Columbus, USA**

J. Alimena, L. Antonelli, B. Bylsma, L. S. Durkin, S. Flowers, B. Francis, A. Hart, C. Hill, R. Hughes, W. Ji, B. Liu, W. Luo, D. Puigh, B. L. Winer, H. W. Wulsin

**Princeton University, Princeton, USA**

S. Cooperstein, O. Driga, P. Elmer, J. Hardenbrook, P. Hebda, D. Lange, J. Luo, D. Marlow, J. Mc Donald, T. Medvedeva, K. Mei, M. Mooney, J. Olsen, C. Palmer, P. Piroué, D. Stickland, A. Svyatkovskiy, C. Tully, A. Zuranski

**University of Puerto Rico, Mayaguez, USA**

S. Malik

**Purdue University, West Lafayette, USA**

A. Barker, V. E. Barnes, S. Folgueras, L. Gutay, M. K. Jha, M. Jones, A. W. Jung, D. H. Miller, N. Neumeister, J. F. Schulte, X. Shi, J. Sun, F. Wang, W. Xie

**Purdue University Calumet, Hammond, USA**

N. Parashar, J. Stupak

**Rice University, Houston, USA**

A. Adair, B. Akgun, Z. Chen, K. M. Ecklund, F. J. M. Geurts, M. Guilbaud, W. Li, B. Michlin, M. Northup, B. P. Padley, R. Redjimi, J. Roberts, J. Rorie, Z. Tu, J. Zabel

**University of Rochester, Rochester, USA**

B. Betchart, A. Bodek, P. de Barbaro, R. Demina, Y. T. Duh, T. Ferbel, M. Galanti, A. Garcia-Bellido, J. Han, O. Hindrichs, A. Khukhunaishvili, K. H. Lo, P. Tan, M. Verzetti

**Rutgers, The State University of New Jersey, Piscataway, USA**

A. Agapitos, J. P. Chou, E. Contreras-Campana, Y. Gershtein, T. A. Gómez Espinosa, E. Halkiadakis, M. Heindl, D. Hidas, E. Hughes, S. Kaplan, R. Kunnawalkam Elayavalli, S. Kyriacou, A. Lath, K. Nash, H. Saka, S. Salur, S. Schnetzer, D. Sheffield, S. Somalwar, R. Stone, S. Thomas, P. Thomassen, M. Walker

**University of Tennessee, Knoxville, USA**

A. G. Delannoy, M. Foerster, J. Heideman, G. Riley, K. Rose, S. Spanier, K. Thapa

**Texas A&M University, College Station, USA**

O. Bouhali<sup>71</sup>, A. Celik, M. Dalchenko, M. De Mattia, A. Delgado, S. Dildick, R. Eusebi, J. Gilmore, T. Huang, E. Juska, T. Kamon<sup>72</sup>, R. Mueller, Y. Pakhotin, R. Patel, A. Perloff, L. Perniè, D. Rathjens, A. Rose, A. Safonov, A. Tatarinov, K. A. Ulmer

**Texas Tech University, Lubbock, USA**

N. Akchurin, C. Cowden, J. Damgov, F. De Guio, C. Dragoiu, P. R. Duderø, J. Faulkner, E. Gurpinar, S. Kunori, K. Lamichhane, S. W. Lee, T. Libeiro, T. Peltola, S. Undleeb, I. Volobouev, Z. Wang

**Vanderbilt University, Nashville, USA**

S. Greene, A. Gurrola, R. Janjam, W. Johns, C. Maguire, A. Melo, H. Ni, P. Sheldon, S. Tuo, J. Velkovska, Q. Xu

**University of Virginia, Charlottesville, USA**

M. W. Arenton, P. Barria, B. Cox, J. Goodell, R. Hirosky, A. Ledovskoy, H. Li, C. Neu, T. Sinthuprasith, X. Sun, Y. Wang, E. Wolfe, F. Xia

**Wayne State University, Detroit, USA**

C. Clarke, R. Harr, P. E. Karchin, J. Sturdy

**University of Wisconsin-Madison, Madison, WI, USA**

D. A. Belknap, J. Buchanan, C. Caillol, S. Dasu, L. Dodd, S. Duric, B. Gomber, M. Grothe, M. Herndon, A. Hervé, P. Klabbers, A. Lanaro, A. Levine, K. Long, R. Loveless, I. Ojalvo, T. Perry, G. A. Pierro, G. Polese, T. Ruggles, A. Savin, N. Smith, W. H. Smith, D. Taylor, N. Woods

† **Deceased**

1: Also at Vienna University of Technology, Vienna, Austria

2: Also at State Key Laboratory of Nuclear Physics and Technology, Peking University, Beijing, China

3: Also at Institut Pluridisciplinaire Hubert Curien, Université de Strasbourg, Université de Haute Alsace Mulhouse, CNRS/IN2P3, Strasbourg, France

- 4: Also at Universidade Estadual de Campinas, Campinas, Brazil
- 5: Also at Universidade Federal de Pelotas, Pelotas, Brazil
- 6: Also at Université Libre de Bruxelles, Bruxelles, Belgium
- 7: Also at Deutsches Elektronen-Synchrotron, Hamburg, Germany
- 8: Also at Joint Institute for Nuclear Research, Dubna, Russia
- 9: Also at Cairo University, Cairo, Egypt
- 10: Also at Fayoum University, El-Fayoum, Egypt
- 11: Now at British University in Egypt, Cairo, Egypt
- 12: Now at Ain Shams University, Cairo, Egypt
- 13: Also at Université de Haute Alsace, Mulhouse, France
- 14: Also at Skobeltsyn Institute of Nuclear Physics, Lomonosov Moscow State University, Moscow, Russia
- 15: Also at Tbilisi State University, Tbilisi, Georgia
- 16: Also at CERN, European Organization for Nuclear Research, Geneva, Switzerland
- 17: Also at RWTH Aachen University, III. Physikalisches Institut A, Aachen, Germany
- 18: Also at University of Hamburg, Hamburg, Germany
- 19: Also at Brandenburg University of Technology, Cottbus, Germany
- 20: Also at Institute of Nuclear Research ATOMKI, Debrecen, Hungary
- 21: Also at MTA-ELTE Lendület CMS Particle and Nuclear Physics Group, Eötvös Loránd University, Budapest, Hungary
- 22: Also at University of Debrecen, Debrecen, Hungary
- 23: Also at Indian Institute of Science Education and Research, Bhopal, India
- 24: Also at Institute of Physics, Bhubaneswar, India
- 25: Also at University of Visva-Bharati, Santiniketan, India
- 26: Also at University of Ruhuna, Matara, Sri Lanka
- 27: Also at Isfahan University of Technology, Isfahan, Iran
- 28: Also at University of Tehran, Department of Engineering Science, Tehran, Iran
- 29: Also at Yazd University, Yazd, Iran
- 30: Also at Plasma Physics Research Center, Science and Research Branch, Islamic Azad University, Tehran, Iran
- 31: Also at Università degli Studi di Siena, Siena, Italy
- 32: Also at Purdue University, West Lafayette, USA
- 33: Also at International Islamic University of Malaysia, Kuala Lumpur, Malaysia
- 34: Also at Malaysian Nuclear Agency, MOSTI, Kajang, Malaysia
- 35: Also at Consejo Nacional de Ciencia y Tecnología, Mexico city, Mexico
- 36: Also at Warsaw University of Technology, Institute of Electronic Systems, Warsaw, Poland
- 37: Also at Institute for Nuclear Research, Moscow, Russia
- 38: Now at National Research Nuclear University 'Moscow Engineering Physics Institute' (MEPhI), Moscow, Russia
- 39: Also at St. Petersburg State Polytechnical University, St. Petersburg, Russia
- 40: Also at University of Florida, Gainesville, USA
- 41: Also at P.N. Lebedev Physical Institute, Moscow, Russia
- 42: Also at Budker Institute of Nuclear Physics, Novosibirsk, Russia
- 43: Also at Faculty of Physics, University of Belgrade, Belgrade, Serbia
- 44: Also at INFN Sezione di Roma; Università di Roma, Rome, Italy
- 45: Also at University of Belgrade, Faculty of Physics and Vinca Institute of Nuclear Sciences, Belgrade, Serbia
- 46: Also at Scuola Normale e Sezione dell'INFN, Pisa, Italy
- 47: Also at National and Kapodistrian University of Athens, Athens, Greece
- 48: Also at Riga Technical University, Riga, Latvia
- 49: Also at Institute for Theoretical and Experimental Physics, Moscow, Russia
- 50: Also at Albert Einstein Center for Fundamental Physics, Bern, Switzerland
- 51: Also at Adiyaman University, Adiyaman, Turkey
- 52: Also at Istanbul Aydin University, Istanbul, Turkey
- 53: Also at Mersin University, Mersin, Turkey
- 54: Also at Cag University, Mersin, Turkey
- 55: Also at Piri Reis University, Istanbul, Turkey
- 56: Also at Ozyegin University, Istanbul, Turkey

- 57: Also at Izmir Institute of Technology, Izmir, Turkey  
58: Also at Marmara University, Istanbul, Turkey  
59: Also at Kafkas University, Kars, Turkey  
60: Also at Istanbul Bilgi University, Istanbul, Turkey  
61: Also at Yildiz Technical University, Istanbul, Turkey  
62: Also at Hacettepe University, Ankara, Turkey  
63: Also at Rutherford Appleton Laboratory, Didcot, UK  
64: Also at School of Physics and Astronomy, University of Southampton, Southampton, UK  
65: Also at Instituto de Astrofísica de Canarias, La Laguna, Spain  
66: Also at Utah Valley University, Orem, USA  
67: Also at Argonne National Laboratory, Argonne, USA  
68: Also at Erzincan University, Erzincan, Turkey  
69: Also at Mimar Sinan University, Istanbul, Istanbul, Turkey  
70: Now at The Catholic University of America, Washington, USA  
71: Also at Texas A&M University at Qatar, Doha, Qatar  
72: Also at Kyungpook National University, Daegu, Korea